Estimating Soil Hydraulic Parameters in Fine-Textured Soils using HYDRUS-1D coupled with PEST

By

Ishmeet Kaur

A Thesis submitted to the Faculty of Graduate Studies of

The University of Manitoba

In Partial fulfilment of the requirements of the degree of

MASTER OF SCIENCE

Department of Biosystems Engineering

University of Manitoba

Winnipeg, Manitoba.

Abstract

Frequent flooding and drought events lead to moisture stress in crops, which leads to poor crop yield and quality. Thus, water management strategies are needed to create a conducive environment for plant growth and performance. An effective strategy requires a long-term understanding of soil moisture dynamics regulated by local soil hydraulic properties and hydrologic factors. This study focused on estimating these soil hydraulic parameters using HYDRUS-1D coupled with PEST (external calibration software) and exploring the non-unique nature of the solution for four growing seasons (2016 –2019). One hundred initial guesses of parameter sets were generated for each year for model calibration. The volumetric soil water contents determined at the site within the 0 - 10 cm, 10 - 30 cm, 30 - 70 cm, and 70 - 130 cm layers over the growing seasons were used to calibrate and validate the models. The statistical parameters used for the evaluation of models were Nash-Sutcliff efficiency (NSE) (0 - 1), Percent bias (PBIAS) (±10%), Ratio of Root Mean Square Error to standard deviation (RSR) (< 0.7) and R^2 (> 0.5). The results showed that PEST was useful in establishing the non-linearity and non-unique nature of the solution, which established that different parameter sets could result in similar performance and, therefore, ascertained the use of a more rigorous approach (maximum likelihood) based on different parameter sets to improve the reliability of the results. The model performance was satisfactory for the simulation of soil water content in 2016, 2017, and 2019 using the calibrated parameter sets. Poor model performance was observed for the 2018 validation period, which showed how the physical manipulation of soil (tillage), physiological stage of the crop, and soil response to weather (shrink-swell) could alter the soil hydraulic properties to a great extent within a season. The results also demonstrated that the saturated hydraulic conductivity varied over the years to about ten times for the topsoil (plough horizon) but was almost constant for deeper soil layers.

Acknowledgements

This thesis would not have been possible without the direct or indirect contribution of several special individuals. This acknowledgement is an opportunity to express my gratitude towards all those who supported me in journeying on this path.

I am deeply indebted to my supervisors, Dr. Ramanathan Sri Ranjan and Dr. Afua Mante for their unwavering support, patience, constant feedback, motivation, belief, and tutelage. I would like to thank my committee members, Dr. Fuji Jian, and Dr. Francis Zvomuya for their invaluable contribution to my research.

I would like to extend my sincere thanks to Dr. Kayla Moore (AAFC), Dr. Timi Ojo (Manitoba Agriculture), Kurt Gottfried (AAFC), Alison Sass (Manitoba Agriculture), and Dr. Nirmal Hari (PESAI) for providing me with the data and information I needed to complete my research.

I am grateful for the funding and scholarship received from NSERC- Discovery Grant, Sustainable Canadian Agricultural Partnership program, University of Manitoba Graduate Fellowship, and the Lord-Selkirk Association of Ruperts Land Agriculture. These funding and awards helped me to achieve personal and professional growth.

I had the pleasure of working with my lab mates: Ifeoluwa Omotade, Thushyanthy Akhileshan, Komlan Koudahe, Dasinija Karikalan, and Mujibur Rahman from Biosystems Engineering. A special thanks to Taurai Matengu for sparing his valuable time for my statistical questions. Thanks to Emmanuel for discussing HYDRUS problems and applications that helped vasting the knowledge.

Words cannot describe the love, affection, and sacrifices of my late mother, Miss Sukhminder, who made me who I am today, personally and professionally. I am so proud to be her daughter. This endeavor would not have been possible without the constant support and encouragement from my incredible husband, Gulbir, and my beloved son, Gurjaap. The confidence shown in me by family members, Mr. Yadwinder, Miss Madanjit, Mr. Rajinder, Miss Herminder, Miss Mohinder, Mr. Balwinder, and their families cannot go unnoticed. I would be remiss not to mention the support from family away from home in Canada, Harmeen and Sakshi.

The belief in me shown by all the contributors has kept my spirits high.

Dedication

To my mother

The late Sukhminder Kaur

Table of Contents

List of Tables

List of Figures

List of Symbols

$\alpha(h)$	Water stress response function
α	Reciprocal of the air-entry value
θ	Volumetric soil water content
θ_r	Residual soil water content
θ_s	Saturated soil water content
h	Soil water pressure head
l	Pore connectivity
K_c	Crop coefficient
K_s	Saturated hydraulic conductivity
n	Pore size distribution index
S	Sink term
S_e	Effective water content
S(h)	Actual root water uptake
S_p	Potential root water uptake rate
Φ	Objective function
^{o}C	Degree Celsius

Chapter 1. Introduction

1.1 Motivation for the research

The agriculture and agri-food sector is one of the most dominant revenue generating industries in Manitoba. It contributed about 7% to the provincial Gross Domestic Product (GDP) by generating $5 billion in 2023 (Manitoba Agriculture, 2024a). About 70% (11.6 million acres) of the total provincial farmland (17.1 million acres) is used for crop production (Statistic Canada, 2023). The province is known to consistently supply safe and high-quality grains, oilseeds, and agri-food products (Manitoba Agriculture, 2023) despite its shorter frost-free season that restricts the choice of crops and growing season. Substantial increase in the plant-based food market from 3.9 billion in 2017 to $8.1 billion in 2023 shows Manitoba continues to meet the soaring demand for crops and crop products (Pierce et al., 2024). Therefore, it is imperative to ensure sustainable crop production.

Climatic patterns and weather highly impact agricultural sustainability. Manitoba has not witnessed high deviations from historical temperatures but is observing seasonal shifts (early springs and longer summers), and high confidence is shown toward the same trend for the future based on reported climatic model projections (Blair et al., 2010; IPCC, 2007). These shifts allow producers to have a wide variety of crop choices. Simultaneously, climatic models predict frequent occurrences of extreme events such as floods, droughts, heat waves, and intense storms (Manitoba Agriculture, 2024d). Over 50% of crop losses are attributed to excess or scarce moisture in Manitoba (Manitoba Agricultural Services Corporation, 2021). These losses and risks can be mitigated using effective and sustainable strategies, which require a better understanding of the structural and hydraulic parameters that influence surface and sub-surface soil water dynamics.

Traditional approaches (experimental) to determining these parameters are laborious, time-consuming, and costly to cover a wider area. The drawbacks associated with the traditional approaches can be mitigated with hydrologic models. Existing models have varying capacities in capturing the soil water dynamics at various depths and with different levels of complexity. Some of these models include Soil Water Atmosphere Plant (SWAP) (Van Dam et al., 1997), Soil-Vegetation-Atmosphere Transfer (SVAT) (Avissar, 1998), Groundwater Loading Effects of Agricultural Management Systems (GLEAMS) (Leonard et al., 1987), and HYDRUS (Šimůnek et al., 2013). Most of these models use Richards equation to simulate water movement through the vadose zone with a comprehensive illustration of soil water content and the fluxes within a model domain. The HYDRUS is one of the most common and successful hydrologic models for simulated soil moisture dynamics based on the Richards equation. HYDRUS requires input data, which include, among others, meteorological data, initial and boundary conditions of the domain, soil physical condition, land use (type of vegetation, root distribution), and physical parameters (saturated hydraulic conductivity, soil water retention curve, and properties affecting the curve) (Šimůnek et al., 2013). Also, model calibration for the physical parameters is necessary to better simulate field conditions. The physical parameters interact with the initial and boundary conditions, necessitating model calibration to ensure the simulation represents field conditions.

As indicated earlier, experimentally determining these parameters is laborious, time-consuming, and costly. Moreover, most experimental methods may not be reliable enough to represent the actual field conditions (Kool et al., 1987). Advancements in computer modelling have made it possible to estimate these complex parameters by making use of readily available soil data from surveys such as soil texture, structure, water content, and matric potential (Kool et al., 1987). Thus, the model is calibrated using these data to optimize unknown parameters through parameter estimation (Kool et al., 1987). This approach leads to an easy, quick, and reliable way to optimize the physical parameters.

Inverse modelling is a popular approach for parameter estimation and is widely used in hydrologic simulations (e.g., Šimůnek et al., 1998; Abd Rashid et al., 2015; Brunetti et al., 2019). Another way is to use external calibration tools such as PEST and UCODE (Doherty et al., 2010a, b; Poeter et al., 1999). Both tools are used to determine a set of parameter optimizations to reduce the difference between simulated and measured values to an acceptable range. Usually, due to the nonlinearity of hydrologic conditions, there may be more than one parameter set that can reproduce the observed data, which makes the solution non-unique and presents a challenge in adopting the data to inform the decision process in developing strategies to address soil water management challenges. The customary practice is to choose the parameters that best fit the evaluation criteria (the least objective function and the best value of statistical evaluation parameters). Still, the best set may not always be the accurate representation of field conditions (Doherty et al., 2010). Also, there could be several models with entirely different sets of parameters that achieve the threshold for the statistical parameter set for performance evaluation. For example, one of two outcomes may result in a better value of Nash-Sutcliff efficiency (NSE), while another outcome gives a better value for the coefficient of determination (R^2). This makes it harder to interpret the model's performance. Thus, adopting a probabilistic approach (maximum likelihood to reproduce the results) to present the outcomes presents a better option to interpret the results (Herrera et al., 2022).

1.2 Problems and gaps addressed in the research

HYDRUS can optimize the physical parameters (hereafter referred to as hydraulic parameters) through inverse modelling provided with a known initial guess of parameters by implementing a

Marquardt-Levenberg-type parameter estimation technique (Šimůnek and Hopmans, 2002). The inverse modelling allows up to 15 parameters to be estimated, but it is not advisable to do so simultaneously (Šimůnek and Hopmans, 2002; Hopmans et al., 2002). This is because of the ill-posed nature of the unsaturated hydraulic condition that can raise non-uniqueness while optimizing these many parameters together (Šimůnek and Hopmans, 2002; Hopmans et al., 2002). ROSETTA is a built-in pedo-transfer model in HYDRUS with a catalogue of different soil types (Šimůnek et al., 2013). However, large discrepancies have been observed between the properties of hydraulic parameters of agricultural soils and ROSETTA values, especially for topsoils (Borek et al., 2021). This may lead to misleading assessments thereby compromising soil water management decisions (Guzman et al., 2015; Tolson and Shoemaker, 2008). Hence, model calibration is critical to improving the reliability of the HYDRUS model. Also, since models are sensitive to the initial guess of parameters, model calibration must be tested with different guesses of initial parameters relevant to the study site. Such approach will generate sets of parameters by applying Markov Chain Monte Carlo Simulation (Herrera et al., 2022). Utilizing PEST supports automating the process of developing multi-calibrated models, which advances our understanding of the non-unique nature of the hydrologic challenge and reliably inform our soil water management decisions (Doherty, 2015).

Previous studies utilizing modelling techniques to advance our knowledge on water management in the province focused on the effect of subsurface drainage on soil water dynamics using HYDRUS (Mante et al., 2017), the impact of controlled, free, and no drainage on Canola yield and oil quality using DRAINMOD (Ndulue, 2022), and compared the effect of four water management strategies (controlled drainage with subirrigation, free drainage with overhead irrigation, no drainage with overhead irrigation, no drainage with no irrigation) (Satchithananantham et al. 2012).

In those studies the hydraulic parameters were estimated using the inverse modelling approach. None of those studies explored the non-uniqueness of the hydraulic parameters. Lack of such information limits our understanding of how local soil hydraulic parameters evolve over time to effectively support water management decisions in the province. Manitoba has a wide range of soil types, soil management practices, agronomic practices, and weather variability. These factors influence the hydraulic parameters, causing their heterogeneity and non-uniqueness. It is imperative that we explore approaches that can support us in accounting for the heterogeneity and the non-uniqueness of the hydraulic parameters to improve our strategies for soil water management in the province.

1.3 Objectives of the research

The main objective of this research was to explore different modelling approaches to estimate soil hydraulic parameters of fine textured soils in Central Manitoba to develop better soil water management strategies.

The specific objectives were to:

- Evaluate the performance of HYDRUS-1D inverse modelling and coupled PEST and HYDRUS-1D in estimating soil hydraulic parameters.
- Determine the maximum likelihood of calibrated parameters based on different parameter sets and their effect on simulation output.

Chapter 2. Literature Review

2.1 Overview of agriculture in Manitoba

Manitoba has a rich history associated with agriculture. Canola, one of the highest-produced crops in Canada, was bred at the University of Manitoba, Winnipeg, Manitoba. The Prairie provinces (Manitoba, Saskatchewan, and Alberta) have the highest proportion of farmland in the country, adding up to approximately 82% of the 62.2 million hectares of farm area in 2021 (Statistics Canada, 2023). Cropland in Manitoba showed an increase of 0.8%, bringing the total cropland area to 11.6 million acres from 2016 to 2019 (Statistics Canada, 2021).

2.1.1 Crops produced in Manitoba

The crops produced in the province in 2021, 2022 and 2023 are shown in Figure. 2.1. Canola, Wheat, and Soybean were the top three seeded and produced crops in 2021 (Statistics Canada, 2021). Crop yield can be significantly affected by weather conditions and management choices such as tillage, crop rotation, and seeding dates (Yang, 2021). It is evident from the reports of Manitoba Agricultural Services Corporation (MASC) that practicing monocropping can reduce crop yield (Kubinec A, 2018). Thus, good planning and adaptation of the choice of crops for rotation is essential for organic and inorganic production systems (Watson et al., 2002). Cultivation of grains, oilseeds and pulses in rotation has shown significant benefits (Yang L, 2021). Spring wheat-canola-soybean is the most practiced crop rotation in Manitoba (Yang L., 2021). The selection of the crops to be sown in the following year depends on profits and disease risks. Canola, soybean, corn, and sunflowers are chosen for their high value and wheat, Barley and Oats are selected as the offset oilseed crops in rotation as they help reduce pests and diseases (Yang L., 2021).

At the site in this study, Soybean-oats-soybean-oats were practiced from 2016 to 2018. Soybean is known to reduce greenhouse emissions as legumes have nitrogen fixation abilities, leading to lower use of nitrogen fertilizers (Qian et al., 2024), enhancing soil fertility, and decreasing diseases from other crops in the cycle (Yang L., 2021). With the push towards plant-based protein, soaring demand and the high market prices of Soybeans are lucrative to farmers and researchers (Voora et al., 2024). As a result, Sustainable Canadian Soy was launched in 2021 and was available from 2023 to growers to work with exporters, industrialists, and researchers to keep pace with the global market (Soy Canada, 2023). Breeders continuously strive to bring drought-resistant varieties to the market to sustain soybean growth (Soy Canada, 2023).

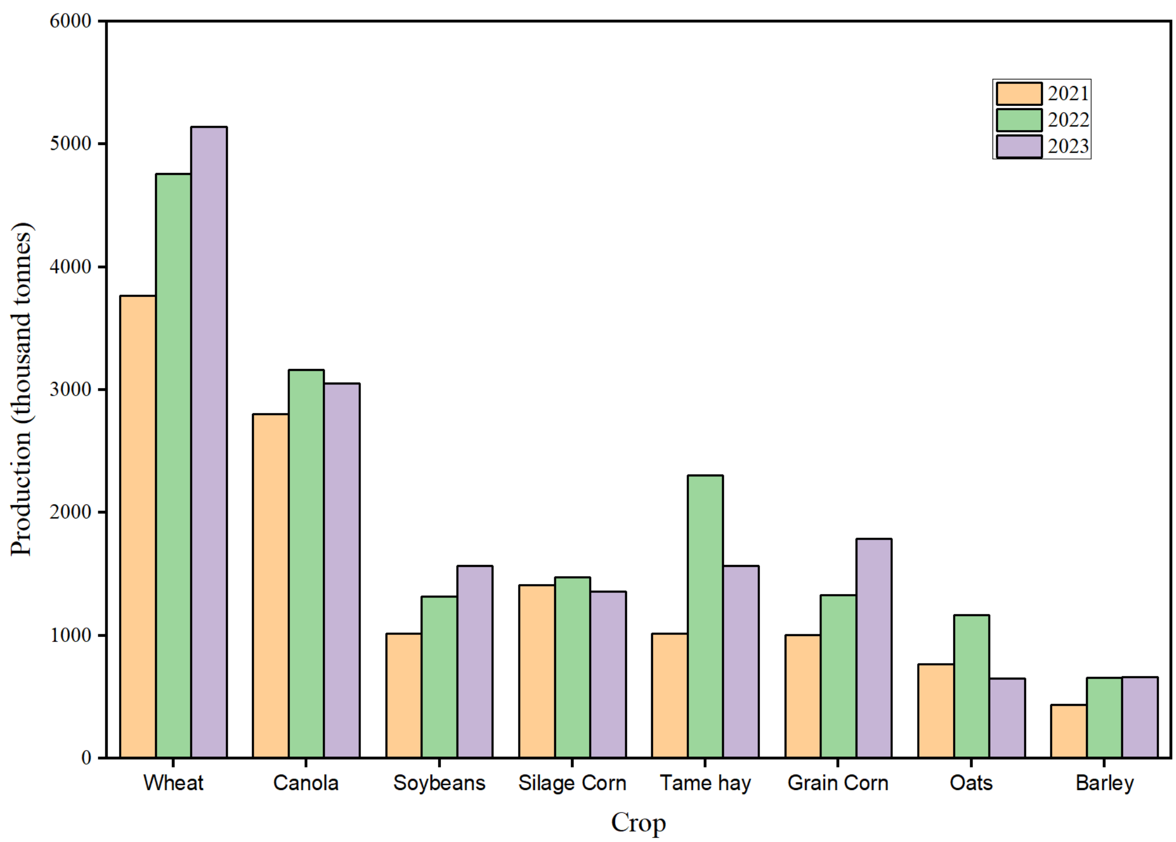

Figure 2.1 Production of selected crops in Manitoba (Source: Statistics Canada, 2024)

In 2022, Manitoba was the second largest producer of Oats in Canada after Saskatchewan, contributing 22.4% to the Country's Oats production (about 1.2 million tons) by setting a record of 116.7 bushels per acre (Manitoba Agriculture, 2023). Also, Oats were one of the top five crops to be exported. The farm cash receipts show that oats and oat products worth $382 million were exported (Manitoba Agriculture, 2024c). The demand for Oats and its products is continuously increasing since a plant-based diet is becoming increasingly popular (Manitoba Agriculture, 2024c).

2.1.2 Contribution of Agriculture to Manitoba's Economy

Agriculture is one of the dominant drivers of Manitoba's economy. Economic activities generated due to crop production can be reflected by its contribution to the region's GDP (Gross Domestic Product). Manitoba's agricultural sector generated 108,000 jobs in the province and generated $5 billion in GDP in 2023 directly and indirectly (Manitoba Agriculture, 2024a). Indirect contribution to the agricultural industry includes milling, processing, and packaging. Crop production alone generated $2.5 billion in GDP in 2023 by directly bringing $6.6 billion in outputs (Manitoba Agriculture, 2024a). Cultivation of soybeans alone aided in generating $835 million in receipts (Manitoba Agriculture, 2024b) The farming industry has not only employed native workers but has benefitted international immigrants also (Statistics Canada, 2023). Canada's farm population is 590710, and immigrants constituted about 7% of the population in 2021 (Statistics Canada, 2023). The agri-food sector in Canada has employed 2.3 million people (AAFC, 2024). Primary agriculture generated $31.7 billion in Canada's GDP, and crop production alone contributed $24.5 billion in 2023 (AAFC, 2024). Manitoba's whole agri-food shared 9.5% of national agri-food exports in 2022 (Manitoba Agriculture, 2023).

2.1.3 Factors Sustaining Farming in Manitoba

Manitoba has abundant land and water resources to augment agricultural areas. Of the total area of 64.7 million ha, about 55 million ha is covered under land (Statistics Canada, 2016). Newdale series of soil, classified as Orthic Black Chernozem, is designated as the provincial soil of Manitoba (Manitoba Forestry Association, 2008). This is a typical grassland soil with a high ratio of organic matter, making it excellent for growing crops (Manitoba Forestry Association, 2008). The topography is mostly nearly levelled (< 2%) (https://agrimaps.gov.mb.ca/agrimaps), making the use of agricultural machinery easy. The second most prominent factor facilitating farming is climate. Manitoba receives a good amount of precipitation through snowfall (winter) and rainfall (summer). At the same time, the melting of snow helps to manage the groundwater table, and both aid in meeting crop water demands.

Manitoba has the third largest area under different farm practices in Canada (Statistics Canada, 2024). The farm practices include crop production, meat, and dairy production. Manitoba has various food and beverage manufacturing and processing plants that make it easier for farmers to sell raw products, resulting in the growth of farmlands (Manitoba Agriculture, 2024e). The province has the world's largest hemp, pea, and bacon processing facilities (Manitoba Agriculture, 2024e). Some of the industries needing crops as their raw materials are Bunge Canada, Viterra, Richardson milling, Roquette and Emerson milling (Grains and Oilseeds), McCain Foods, and Simplot Canada (potatoes) (Manitoba Agriculture, 2024e).

Another factor boosting the industry is the increasing number of young farmers involved with agriculture. Manitoba has the most farmers under 35 who bring innovation, education, and excellence to the profession (Manitoba Agriculture, 2023). Some initiatives to attract young farmers are the Manitoba Young Farmers Conference, the Canadian Young Farmers' Forum, and the Young Farmer Rebate.

Manitoba Agriculture, Diversification Centres, the University of Manitoba Faculty of Agricultural and Food Sciences, and others do world-class research addressing existing and emerging challenges (Manitoba Agriculture, 2024). Research agencies provide good funding to attract researchers (Manitoba Agriculture, 2024). For example: The Sustainable Canadian Agricultural Partnership allocated $221 million to support research in Manitoba (Manitoba Agriculture, 2019) . Many initiatives have been taken to increase productivity at the farm level through breeding, developing rotational plans, strategies such as Sustainable Canadian Soy (2021), Manitoba Protein Advantage Strategy (2019), and developing mobile applications to help farmers get real-time data from the field.

2.1.4 Challenges and risks associated with farming in Manitoba

One of the priority areas identified by researchers in Canada is water management, and funding is allocated to implement practices related to irrigation efficiency, drainage water management, water use efficiency and water supply (Manitoba Agriculture, 2021). Ndulue (2022) found that water management system performance is significantly affected by local weather. The weather changes predicted by the climatic models bring more unpredictability to floods and drought due to climate change. Climate change refers to long-term changes in temperature, precipitation, and weather patterns (Riedy, 2016). Bekalu et al. (2021) listed various climatic models to project future scenarios. They predict shorter and warmer winters because of global greenhouse gases. Other projected changes are the increased frequency of extreme climatic events, such as intense but acute rainfall, leading to frequent floods and droughts (Manitoba Agriculture, 2024d).

The longer summers undoubtedly result in a longer growing season that helps farmers to have more options to choose crops that were earlier restricted by the shorter growing season and cultivate multiple crops per year (Sauchyn and Kulshreshtha, 2008). It should be noted that warmer summers may result in heat stress leading to decreased crop productivity (Climate Change Connection, 2013). Shorter winters will trigger early spring melting, resulting in high soil moisture and moisture deficit in the mid-season (Climate Change Connection, 2013).

Excess or scarce soil moisture can affect plant growth and performance by impacting the aeration around the roots, water, and nutrient uptake and can reduce the yield (Osborne et al., 2003; Cordeiro, 2014). The former also affects the planning of field operations, as working on wet soil can increase the risk of soil degradation and losses through soil compaction and erosion (Müller et al., 2011; McKenzie, 2010) and delay planting dates. A delay in the planting till the start of June could reduce the crop yield by 20-30%, depending on the crop (Ndulue, 2022). Compaction inhibits all soil functions and processes, detrimental to sustainable crop production and a healthy environment (Shaheb et al., 2021). Draining excess water ensures timely accessibility to the field and reduces the risk of compaction or structural damage (Mante et al., 2018). Also, excess soil moisture promotes diseases (Sadras et al., 2016), for example, flooded soybean is prone to diseases spread by cyst nematode and white mould, such as sudden death syndrome (Staton, 2014), whereas water deficit can reduce the cell water potential and wilt the plants (Zhang et al., 2020). However, most of the drainage contractors in Manitoba adopt drainage design variables from other regions that fail to achieve agronomic, economic, and environmental gains. Thus, the existing drainage systems should be better designed to accomplish the goals (Ndulue, 2022). Ndulue (2022) suggested drain spacing of 15 m is beneficial for crops. However, Mante (2017) found that drain spacing wider than 12 m can be vulnerable to soil compaction in Manitoba. Hence, the factors affecting the drainage systems, i.e., soil hydraulic properties, should be thoroughly explored.

2.1.5 Economic loss to the Ag industry due to soil moisture challenges

Moisture stress can significantly affect soil quality by clogging the soil, eroding the top layer, shrinking, and swelling, leading to preferential flows and affecting soil's physical, chemical, and biological activity (Al-Kaisi, 2017). Excess water content could result from high snowmelt, rainfall, high water table, over-irrigation, and poor drainage. In contrast, water content scarcity is likely caused by less precipitation, inadequate irrigation, and high evaporation. Along with the intensity of the event, the effect is attributed to the soil texture, environmental conditions, and soil disturbance history (Patel et al., 2021). Sandy soils would be more sensitive to droughts, whereas clay soils can be waterlogged.

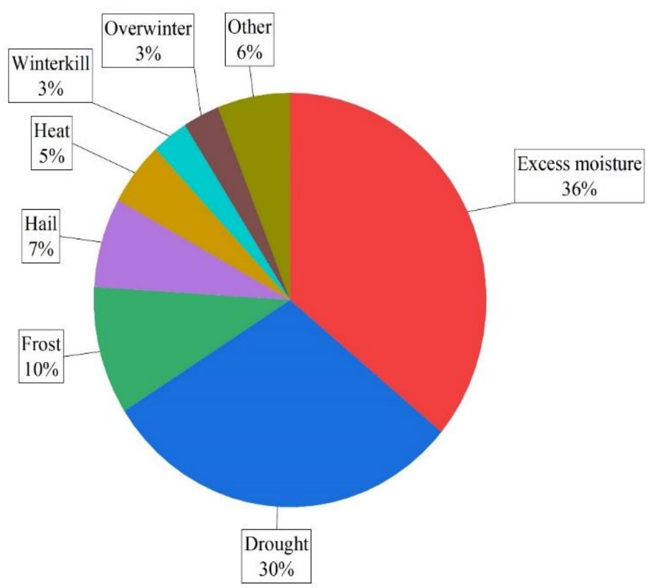

Figure 2.2 Historical Causes of Loss (1996-2021) (MASC, 2021)

Occurrences of floods and drought events in the agriculture sector are the most significant natural hazards. More than 2-3rd of the crop losses occurred because of moisture extremes (fig. 2.2) in

Manitoba. Assiniboine river floods in 2011 directly resulted in 73% of crop losses (Asante et al., 2021). Excess flooding can result in a high amount of fertilizer application as runoff occurs considerably (Asante, 2021). This nutrient migration led to the Eutrophication of Lake Winnipeg and groundwater pollution, resulting in a denitrification cost of $500 million. About $42 million was allocated as reduced soil trafficability resulted in about 3 million acres of land unsown (Asante et al., 2021).

Contrary to that, the recent agricultural drought of 2021 resulted in a direct loss of $75 million in crop sales. However, some of this loss was covered by higher prices of crops otherwise the estimated drought impact could be $1.4 billion (Province of Manitoba, 2021). The agriculture industry was the most impacted. Additionally, this drought reduced $47 million in provincial GDP and 267 jobs (Province of Manitoba, 2021). The crop insurance payment peaked at $469 million from $62 million in 2020, an increase of 455% from the previous five-year average (Province of Manitoba, 2021).

Some indirect effects of moisture extremes on the economy are crop yield losses caused by factors such as Compaction, soil erosion, etc. Working on the wet fields increases the risk of compaction in the agricultural fields, further impeding crop root growth and reducing aeration and water flow. This restricted growth and access to air and water would adversely affect the crop yield (AAFC, 2024). Lack of aeration in the soil caused by excess moisture can result in a reduced number of beneficial microbes. This makes it harder for the crop to absorb nutrients such as phosphorus (AAFC, 2024). Even after adopting conservation agriculture, the nationwide crop yield losses due to soil erosion are estimated to be around $3.1 billion annually by Dr. David Lobb (Soil Scientist, Department of Soil Science, University of Manitoba) (Wichers, 2019).

One of the main problems of soil degradation in Manitoba is salinization, and soil Salinity in the field is directly linked to water management (Franzen et al., 2024). The crop gets injured by excessive salts interfering with the crop water and nutrient uptake (Franzen et al., 2024). Salinity can lead to up to 25% yield losses at the salinity level of 1.8 dS/m.

2.2 Risk Mitigation

The previous section highlights the fact that excess or deficit of soil moisture can jeopardize Manitoba's agriculture and, hence, GDP. The encroaching climate change brings more unpredictability to floods and drought occurrences (Manitoba Agriculture, 2024d). Therefore, producers, researchers, industries, and government organizations are striving to alleviate the adverse effects of these occurrences by educating and adapting Beneficiary Management Practices at farm levels to a global scale (The Senate of Canada, 2024; Manitoba Agriculture, 2024)

The University of Manitoba has introduced various soil and water management, irrigation, drainage, and remediation courses, constantly updating the curriculum to advance students understanding of sustainable practices (University of Manitoba, 2024). The highest proportion of young farmers in Manitoba discussed in the previous section in Manitoba is one of the outcomes.

Different strategies should be obtained to regulate soil water content depending on drought or flood conditions. Management strategies for droughty states aim to conserve or increase soil water content. They involve the following but are not limited to:

(i) Abstaining from summer fallow as it lowers the soil organic matter and leaves soil susceptible to erosion and evaporation,

(ii) Adopting reduced tillage and preventing unnecessary tillage from leaving crop residues to conserve moisture.

(iii) Adopting irrigation methods to meet crop water requirements. (Manitoba Agriculture, 2008)

Contradictory to the above steps, management strategies for wet extremes aim toward the removal of excess water. Asante et al. (2021) identified the standard on-farm practices in Manitoba as land grading, wetlands, groundwater and pumps, cover crops, water reservoirs, mole drainage, open ditches, and tile drainage systems. Among these, the best management strategy is decided based on the event's intensity, the farm's size, and the soil texture (Asante et al., 2021). Water reservoirs, tile drainage, land grading, and cover cropping are the four management practices proposed based on Manitoba's heterogeneous soils, crops, climate, and long-term benefits and reported to be profitable over time (Asante and Ashton, 2021).

There is a close relationship between adaptation and mitigation. Producers are funded to adopt the Beneficiary Management Practices by incorporating new and sustainable on-farm practices such as the selection of high tolerant seed varieties, crop rotations, mixed farming, installing proposed water management systems, cover crops, and organic amendments by working in close relationships with researchers, industries and government (Manitoba Agriculture, 2024).

Manitoba Agriculture, Agriculture and Agri-Food Canada (AAFC), Manitoba Crop Alliance (MCA), Manitoba Pulse and Soybean Growers (MPSG), and Manitoba Canola Growers Association (MCGA), among others, are constantly developing projects, policies, strategies, guidelines, and programs to address the soil water issues. Global Water Futures initiated a seven-year pan-Canadian research project to deliver risk management solutions for the improvement of Canada's water resources for agriculture (Merrill et al., 2019). Additionally, MCA, MPSG, MCGA have funded and collaborated with AAFC Brandon, Brandon University and the University of Manitoba on the 'Extremes of Moisture' project that is made up of various sub-projects to understand crop responses and mitigation of losses (MCA, 2024). They acknowledge that the result of one management strategy differs from site to site depending upon the soil texture, climate, and cultivation. Real-time in situ soil monitoring (Dr. Paul Bullock's research group in the Department of Soil Science, University of Manitoba) and testing of controlled tile drainage with back splashing of water is one of the sub-projects (Dr. Ramanathan Sri Ranjan's research group in the Department of Biosystems Engineering, University of Manitoba). A recent project supported by the commodity groups and the Sustainable Canadian Agricultural Partnership is a research project on "building resilient soils in Manitoba" led by Dr. Afua Mante's research group in the Department of Soil Science, University of Manitoba (Manitoba Crop Alliance, 2024).

Losses due to droughts (Figure. 2.2) show that supplementing water application is as vital as drainage systems to maintain agricultural systems. Controlled drainage is a cost-effective water management tool (Christianson et al., 2016) that can retain water in the soil profile by reducing the amount of water discharged. During seeding or harvesting, the excess water can be discharged freely, but plants can take the retained soil water at other times during dry times (PAMI, 2018). Controlled drainage with sub-irrigation (CDSI) is in its preliminary stages in the province. Tan et al., 1999 found that sub-irrigating with tile water improves crop yield in Ontario, while Satchithanantham (2012) observed no significant impact on potato yield with CDSI in 2010 in Southern Manitoba. This variation can be attributed to soil type, climate, and management. Ndulue (2022) suggests re-examining the design and operation of the existing drainage system in Manitoba. He added that adopting drainage design variables from other regions without information on site-specific conditions may not bring desirable benefits. Thus, a site-specific study on soil water dynamics should be conducted.

2.3 Soil water dynamics

Soil water dynamics require a basic understanding of the hydrological cycle, which comprises different components including but not limited to precipitation, infiltration, percolation, evaporation, transpiration, and run-off (Ndulue, 2022). Once the water reaches the ground, the water distribution depends on the ability of soil to infiltrate, retain and move the water. Nevertheless, it also depends on the intensity of rainfall. Evapotranspiration depends on climatic variables such as solar radiation, wind, temperature, humidity, and plant characteristics. Manitoba's diverse soil and climate make relying on average soil-plant-water interactions impossible. The water uptake pattern of plants affects transpiration rates, which depend on the availability of moisture in the soil and the potential contribution from groundwater. Up to 18% and 92% contribution from the groundwater towards consumptive use was observed under maize and potato (Babajimopoulos et al., 2007; Satchithanantham et al., 2012). Thus, to understand soil water dynamics accurately, knowledge of all the above-written parameters is crucial.

FAO-PM equation is widely accepted for estimating reference evapotranspiration but requires many input variables (Allen, 1998). Considering the high spatial weather variability in Manitoba, most of the parameters needed in the equation are not available locally at all the weather stations. Furthermore, data on soil physical parameters and groundwater are limited. This limitation makes it challenging to study the soil water dynamics and develop strategies to address soil water challenges in Manitoba.

2.4 Soil water and weather monitoring

Considering the essence of high-quality weather data, Manitoba Agriculture has been expanding the weather monitoring network constantly. As a result, 63 new stations were installed from 2015-17 (Ojo and Manaigre, 2021). Currently, it operates about 120 automated near real-time permanent weather stations complementing the weather stations of Environment Canada and other networks. Most of them ensure coverage of about 1 in 30 km located at the edge of the cropped areas (Ojo and Manaigre, 2021). Each station measures minimum and maximum air temperature, relative humidity, rainfall, wind speed and direction, soil temperature and water content, and solar radiation at 15-minute intervals.

Canadian Drought Monitor (CDM), operated by Agriculture and Agri-food Canada, provides monthly drought assessments throughout the country. They classify drought based on precipitation percentile and return period into five classes ranging from abnormally dry to exceptional drought (AAFC, 2024).

Table 2.1 Classification Scheme for Canadian Drought Monitor (AAFC, 2024).

Class	Severity	Return Period
D0	Abnormally Dry	1 in 3-year event
D1	Moderate Drought	1 in 5-year event
D2	Severe drought	1 in 10-year event
D3	Extreme Drought	1 in 20-year event
D4	Exceptional Drought	1 in 50-year event

AAFC and Environment and Climate Change Canada collaborated and installed 15 soil moisture monitoring stations in 2010 and 2011 in Manitoba as a part of the Sustainable Agriculture Environmental Systems project '*Earth Observation Information On Crops And Soils For Agreed Environmental Monitoring In Canada.'* The stations are called *Real Time In Situ Soil Monitoring For Agriculture* (RISMA) networks (Pacheco et al., 2014) (Figure 2.3). The data from these stations is used to calibrate and validate the remote measurement and modelling results.

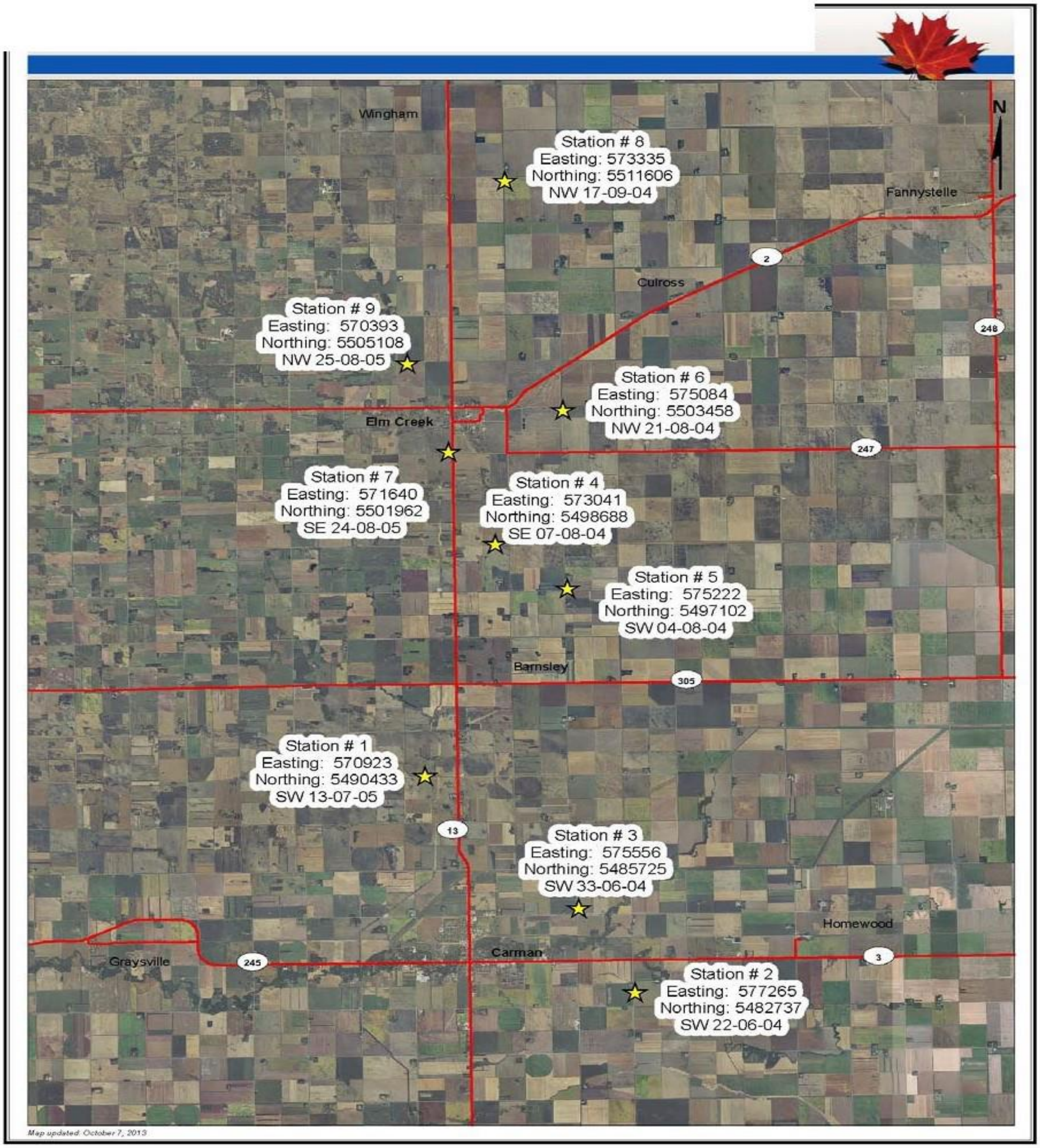

Figure 2.3 Map of RISMA stations in the Carman area (Pacheko et al., 2014)

A detailed description of the site selection process and installation procedure is provided by Walker (2012). The soil moisture data is complemented by meteorological sensors that measure air temperature, humidity, wind speed, and direction. To accurately represent the cropped area, three soil moisture sensors are installed within the field, about 6-30 cm from the edge at 0-5 cm, 5 cm, 20 cm, 50 cm, and 100 cm at each depth. AAFC personnel carefully seed and harvest the crops near the sensors to ensure sensor safety and better imitate the field conditions. A complete re-installation of the sensors was performed at MB5 in 2014 following sensor malfunction (Powers, 2014). This study uses data from the same station from 2016 to 2019.

2.4.1 Limitations with monitoring stations

Most Manitoba-Ag weather stations measuring soil water content are installed outside the cultivated crop, either seeded to grass or native grass. Understanding the soil moisture dynamics under a specific crop makes it challenging. RISMA stations overcome this challenge as the sensors are installed within the cultivated area. However, they do not provide data on solar radiation and groundwater table depth, which are crucial in assessing soil water dynamics. A critical assessment of local soil water dynamics and a simulation of future scenarios will support the development of strategies for water management.

2.5 Simulation of soil water dynamics

Agricultural modelling is an easy and quick way to study historic, present, and future soil and water resources management events. They have been instrumental in addressing issues such as water management, salinization, and environmental contaminants (Burges, 1986). Advancements in technology have led to significant development in computer modelling to support flood monitoring, assessment of climate change effects, watershed management, water resource management, and evaluation of soil water dynamics (Cherif et al., 2023; Singh and Woolheiser, 2002). Some of the models that can simulate water and nutrient flow in variably saturated media are ENVIRO-GRO (Feng et al., 2003), SALTMED (Ragab et al., 2005), UNSATCHEM (Suarez and Šimůnek, 1997), SWAP (Van Dam et al., 1997), HYDRUS 1D/2D/3D package. The water flow through the unsaturated media in most models is governed by the Richards equation (Šimůnek et al., 2013). All these mentioned models, except the HYDRUS package, are one-dimensional and simplify the flow into vertical dimension only. The HYDRUS package provides flexibility to simulate the flow in one, two or three dimensions (Šimůnek et al., 2018). HYDRUS 1D/2D/3D packages have been demonstrated to perform reasonably well for simulating water flow in sandy loam soils under potato cultivation in Manitoba (Mante et al., 2017), simulating water flow along with the phosphorus transport (Qiao 2014), simulation of water flow in water repellent soils (Wang, 2018), simulating water and saline dynamics in unsaturated soils in semi-arid regions of Tunisia with different water qualities (Kanzari et al., 2018). Suleiman (2008) compared and validated soil water dynamics simulation results in vertical drainage experiments. The present study uses the HYDRUS package to simulate the vertical water flow.

2.5.1 HYDRUS-1D Numerical Modelling

Water flow in the vadose zone in HYDRUS-1D is governed by the Richards equation (Equation 2.1) (Šimůnek et al., 2013).

$$\frac{d\theta}{\mathrm{d}t} = \frac{\partial}{\partial x}\left[K\left(\frac{\partial h}{\partial x} + \cos\alpha\right)\right] - S \qquad 2.1$$

Where h is the water pressure head [L], θ represents Volumetric Water content [L^3L^{-3}], t is time [T], x is spatial co-ordinate (positive upwards and negative downwards), K is unsaturated hydraulic conductivity [LT^{-1}], α represents the angle between the vertical axis and direction of flow movement to be studied, and S = Sink term [$L^3L^{-3}\,T^{-1}$].

The model assumes a negligible impact of air phase and thermal gradients in the water flow in the variably saturated media (Šimůnek et al., 2013). It allows the use of five different analytical models to be followed for soil hydraulic parameters: Brooks and Corey (1964), van Genuchten (1980), Vogel and Cislerova (1988), Kosugi (1996), and Durner (1994. Van Genuchten-Maulem's hydraulic model was implemented in this study to describe the unsaturated hydraulic properties as the HYDRUS code uses the set of closed-form equations resembling van Genuchten (1980). Equations 2.2 to 2.5 represent the expressions derived by Van-Genuchten (Šimůnek et al., 2013).

$$\theta_h = \begin{cases} \theta_r + \dfrac{\theta_s - \theta_r}{[1 + |\alpha h|^n]^m} & h < 0 \quad (2.2) \\ \theta_s & h \geq 0 \quad (2.3) \end{cases}$$

$$K(h) = K_s S_e^l \left[1 - \left(1 - S_e^{1/m}\right)^m\right]^2 \tag{2.4}$$

$$m = 1 - \frac{1}{n}, n > 1 \tag{2.5}$$

Where h is the air entry value [L], θ_r represents the residual water content [-], θ_s is the saturated water content of the soil [-], α, m and n are soil-dependent empirical parameters [L^{-1}], [-], [-] representing inverse-air entry value (α) and pore size distribution index (n), S_e is the effective water content [-], K_s is the saturated Hydraulic conductivity [LT^{-1}], KR is the relative hydraulic conductivity, K(h) is the unsaturated hydraulic conductivity at the pressure head h [LT^{-1}], l is the poor connectivity parameter (Mualem, 1976). Hence, θ_r, θ_s, α, n, K_s, l will be termed as vG parameters in the study.

The model requires the values for vG parameters as one of the inputs to simulate the water flow accurately.

2.6 Parameter estimation

Calibrating a model is a primary step towards the modelling process. It becomes an integral part of training a model for the site-specific simulations. In general, calibration aims to mimic the hydrologic process by altering the parameters and ensuring their meaning and importance. Model calibration is attained by training a model with already measured data and then simulating it for the rest of the period (Simunek and Hopmans, 2002). HYDRUS codes require little or no calibration when the parameters (residual and saturated water content, saturated hydraulic conductivity, and empirical constants) are known. Thus, these parameters need to be determined or estimated to accurately simulate the field conditions. These parameters can be determined by direct or indirect methods.

2.6.1 Direct methods

Residual, saturated water content, Saturated hydraulic conductivity, and water retention can be measured directly. In contrast, α and η are the empirical constants based on the water retention curves described in section 2.5.

The soil water retention curve can be determined by plotting suction tables. This includes recording the water content in the soil at different suctions, which was implemented by Ramos et al. (2011). Residual water content is the lowest water content in the soil at infinitely high matric potential or when the gradient ($d\theta/dh$) becomes zero (Geo-Slope International Ltd, (2015)). This can be recorded while plotting the suction tables. Saturated water content is the maximum amount of water stored in the soil matrix. This can be determined by observing the water content of the soil at saturation, i.e., no more water can be absorbed by the soil (Eslamian et al., 2018). Saturated hydraulic conductivity is one of the most difficult parameters to measure (Diminescu et al., 2019) and is highly variable (Warrick and Neilsen, 1980; Wilding and Drees, 1983). It can be measured either in the laboratory or in the field. The laboratory method requires undisturbed sampling. Collecting undisturbed samples from deeper depths is hard, especially in rocky soils. Diminescu et al. (2019) compared five laboratory methods including variable head permeameter - Kamenski, simplified permeameter, constant-head Cromer permeameter, and constant–head permeameter connected to piezometric tubes. They found that constant head permeameter connected to piezometric tubes performed the best for sand. It gets difficult to maintain a constant flow rate to maintain the constant heads in materials with low hydraulic conductivity, such as clay soils (Woessner et al., 2020). Field methods include double-ring infiltrometer tests, Guelph permeameter, and air entry permeameter (Lee et al., 1985).

These direct methods have several limitations, like being time-consuming, expensive, and requiring some conditions, such as steady state or equilibrium hydraulic conditions (Kool et al., 1987). However, these methods are instantaneous and would not be advisable to rely on for long-term studies. Also, hydraulic conductivity measurements made in the laboratory or in situ are restricted to the applications related to the processes at that same scale (McKenzie et al., 2002).

2.6.2 Indirect methods

Over the years, many indirect methods have been developed to estimate these hydraulic parameters and their relationships. When the calibration of the model is performed to achieve the parameter values, it is termed 'Parameter Estimation' (Eden et al., 2014).

The parameter estimation technique uses inverse modelling, where the parameters are estimated using readily available data such as soil texture, bulk density, water content, particle size distribution, etc. (Kool et al., 1987). Increasing applications of inverse modelling (Kool et al., 1987; Hudson et al., 1991) indicate various advantages of parameter estimation methods compared to direct measurement techniques.

Advantages of Parameter estimation over direct methods:

- The need to mathematically invert numerical equations is eliminated

- We can estimate the hydraulic properties/hydraulic conductivity of a full range of water contents.
- It can be used with ease on layered soils.
- Can estimate many hydraulic properties of different layers simultaneously
- Can estimate the parameters in history, present and future.

While parameter estimation techniques possess several advantages, many problems of convergence, parameter uniqueness, and computational efficiency remain unsolved.

2.6.2.1 Calibration via HYDRUS-1D Inverse modelling

HYDRUS-1D has a built-in calibration method based on Marquardt-Levenberg method (Marquardt, 1963). It provides a catalogue of 12 textural soil classes to provide an initial estimate of soil hydraulic parameters (Carsel and Parrish, 1988) and the pedotransfer functions using the ROSETTA program developed by Schaap et al. (2001) (Šimůnek et al., 2012). However, large discrepancies were reported (about four times) in the saturated hydraulic conductivity value estimated by ROSETTA and in-situ measurement in Poland (Borek et al., 2021). Thus, the uncertainty in the initial estimated parameters may result in questioning of the calibrated parameters. Also, the HYDRUS-1D inverse modelling code restricts the maximum number of optimizable parameters to 15. Thus, in problems of optimization of more than 15 parameters, either the code needs to be varied or some parameters need to be fixed manually, though it is not recommended to optimize that many parameters (Šimůnek and Hopmans, 2002; Hopmans et al., 2002). HYDRUS Thus, it becomes hard to optimize the parameters considering the heterogeneity of agricultural soils. Hence, there is a need to couple HYDRUS with an external calibration tool to calibrate the model effectively.

2.6.2.2 Calibration with External software

Several reliable calibration methods in conjunction with HYDRUS-1D have been used since the 2000s. A brief overview of PEST, UCODE, GA, NSGA-II, MOSCEM-UA, and AMALGAM-Multi-objective Optimization Algorithm is provided by Wang (2018).

PEST and UCODE were found to be highly efficient computationally. However, PEST is freely available and does not require any computer language proficiency. PEST is a non-linear parameter estimation program that works with another hydrologic model with a Windows-based interface to calibrate the model (Doherty et al. 1995). PEST is linked with a model with the help of a user-created template, instruction, and control files that guide it in changing the input parameters, respecting the bounds, and reading output from the model output files. It runs the model, compares the outputs to the observations (measured values), adjusts selected parameters using the defined optimization algorithm, and reruns the model until the preset criterion is met. The preset criterion could be the agreement between model outputs and observations or the number of iterations.

Once optimized, the parameters are validated using a two-step calibration scheme or split sampling. It involves dividing the data into two datasets, where one dataset is used to calibrate the model (calibration). In contrast, the other is used to compare the measured data using the parameters (Šimůnek and de Vos, 1999). The model is accepted if it predicts the system response during validation within acceptable limits of the evaluation criteria (Anderson and Woessner, 1991).

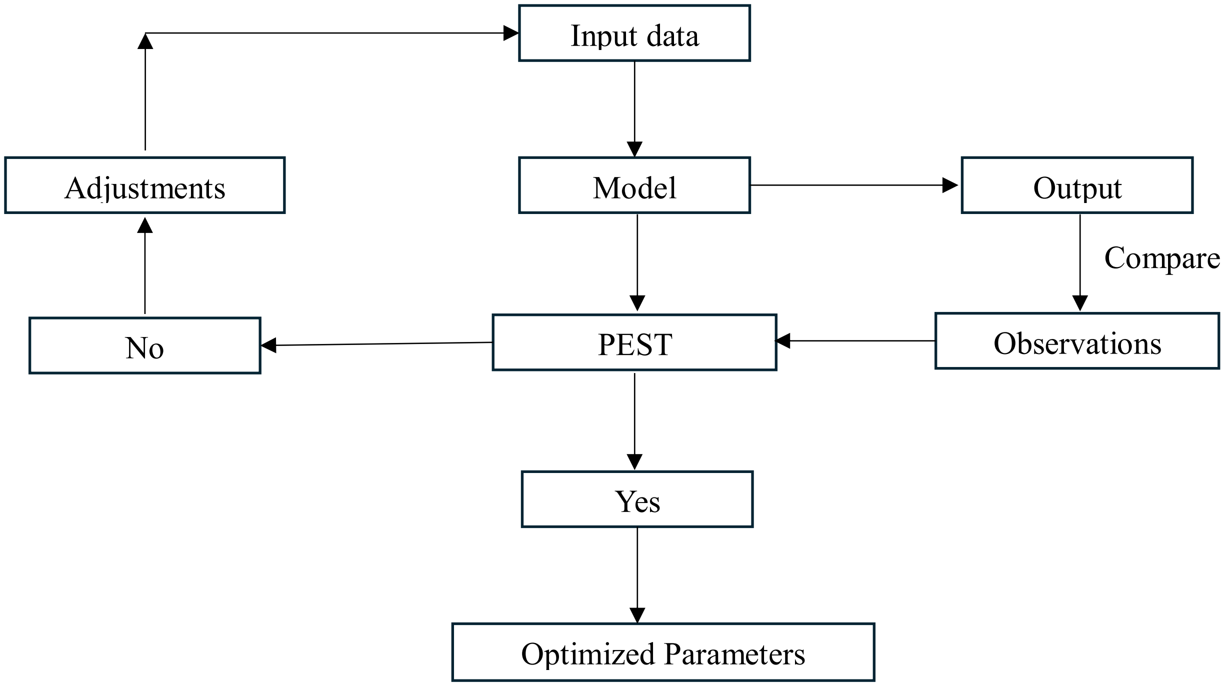

Figure 2.4 Flowchart showing PEST-Model layout

2.7 Model evaluation

Model evaluation is critical to determine model performance in simulating conditions (Harmel et al., 2014; Bennet et al., 2013). This can be attained by comparing the simulated outputs from the model and field or laboratory observations. The most common, easiest, and initial test for hydrological simulations is to plot and visually compare the simulated and observed trends. However, just the visual comparison is insufficient to conclude the model's goodness as the visual differences and their interpretation depend highly on the axis scale and are susceptible to human error. Statistical approaches, including Pearson's correlation coefficient (r), Coefficient of determination (R^2), Nash-Sutcliff efficiency, PBIAS and, Root mean square error (RMSE) are used to achieve rigor in the evaluation process (Moriasi et al. 2012).

2.7.1 Pearson's correlation coefficient (r) and coefficient of determination (R^2)

The coefficient of determination describes the fraction of variance in observed data explained by the model. It ranges from 0 to 1, and the higher the R^2, the lesser the error variance. R^2 more than 0.5 indicates satisfactory performance of the model. The correlation coefficient quantifies the linear relationship between observed and simulated values. It ranges from -1 to 1; the former implies a perfect negative linear relationship, and the latter shows a perfect positive one. Values in proximity to 0 indicate a non-linear relationship.

$$R^2 = (r)^2 \tag{2.6}$$

$$r = \frac{n\,\Sigma_{i=1}^{n}(y_i^{obs} * y_i^{sim}) - (\Sigma_{i=1}^{n} y_i^{obs})(\Sigma_{i=1}^{n} y_i^{sim})}{\sqrt{[n\,\Sigma_{i=1}^{n} {y_i^{obs}}^2 (\Sigma_{i=1}^{n} y_i^{obs})^2]\,[n\,\Sigma_{i=1}^{n} {y_i^{sim}}^2 (\Sigma_{i=1}^{n} y_i^{sim})^2]}} \tag{2.7}$$

2.7.2 Slope and y-intercept

The slope of the best-fit line in the plot of simulated data vs observed data indicates the deviation between the two datasets. In other words, it tells how well the two datasets match. The intercept in the equation means the lead or lag between the predicted and actual values. The slope (m) of 1 and intercept (c) of 0 indicates that the model perfectly mimicked the exact values.

$$y_i^{sim} = m(y_i^{obs}) + c \tag{2.8}$$

2.7.3 NSE

The Nash-Sutcliff efficiency is a dimensionless quantity used to determine the goodness of fit between the simulated and observed values recommended for use by ASCE (1993) and Legates and McCabe (1999). It can range from -∞ to 1. NSE above 0.5 is acceptable for modelling, and a figure of more than 0.75 indicates a very good model performance. In other words, it showed the tendency of a model to fit a 1:1 line.

$$\mathrm{NSE} = 1 - \left[\frac{\Sigma_{i=1}^{n}\left(y_i^{obs} - y_i^{sim}\right)^2}{\Sigma_{i=1}^{n}\left(y_i^{obs} - y_i^{mean}\right)^2}\right] \quad 2.9$$

2.7.4 PBIAS

The percent Bias is the percentage measure of the tendency of the predicted value to be greater or smaller than the observed value. As the percentage measure ranges from -100 to 100, where 0 is considered optimal. Positive values indicate model underestimation, and negative values indicate the model overestimates. In other words, the closer the PBIAS is to 0.0, the higher the model accuracy.

$$\mathrm{PBIAS} = \left[\frac{\Sigma_{i=1}^{n}\left(y_i^{obs} - y_i^{sim}\right) \times 100}{\Sigma_{i=1}^{n}\left(y_i^{obs}\right)}\right] \quad 2.10$$

2.7.5 RMSE

The root mean square error (RMSE) is another error-measuring index measuring the deviations between observed and simulated values, and it has the same units as the observed data. Model outputs resulting in RMSE equal to 0 are perfect. RMSE is always a positive value; the lower the RMSE, the better the model.

2.7.6 RSR

The RSR is the ratio between root mean square error and standard deviation. A lower RSR value implies a lower RMSE and better model performance. RSR equal to 0.7 is considered satisfactory.

$$\mathrm{RSR} = \frac{\mathrm{RMSE}}{\mathrm{Standard\ deviation}} = \frac{\sqrt{\Sigma_{i=1}^{n}\left(y_i^{obs} - y_i^{sim}\right)^2}}{\sqrt{\Sigma_{i=1}^{n}\left(y_i^{obs} - y_i^{mean}\right)^2}} \quad 2.11$$

In all the equations from 2.6 to 2.8,

y_i^{obs} = ith measured/observed value for the element being evaluated.

y_i^{sim} = i^{th} simulated value for the element being evaluated

y_i^{mean} = mean (average) value for the element being evaluated

2.8 Parameter non-uniqueness

The performance and reliability of flow simulations with hydrologic models are questioned by the uncertainties in the modelling (Herrera et al., 2022). These uncertainties may result from soil heterogeneities, human errors, lack of information, model structures, observation errors, and poor understanding of natural phenomena (Moges et al., 2021; Pechlivanidis et al., 2011). Also, the parameter estimation process using inverse modelling can lead to additional uncertainties, which may arise when the solution is unstable, non-unique or impossible (Herrera et al., 2022). As hydrologic problems are primarily non-linear, non-uniqueness often occurs (Doherty, 2015). The solution is usually selected based on the best objective function. It should, however, be noted that sets of parameters can result in equally good objective function (Herrera et al., 2022). The frequent cause of these ill-determined problems is the correlation among the parameters (Doherty, 2015). In the case of high correlation, a change in one parameter gets balanced by the change in the other parameter, resulting in several solutions with acceptable objective functions (Doherty, 2015). Also, in field studies, direct comparisons of model performance by defining simple and best objective functions may not be realistic (Abbaspour, 2022). The probabilistic approach to represent the model results is better (Herrera et al., 2022).

Multiple calibrations can be performed to explore the non-uniqueness of the given hydrologic scenario by generating a number of parameter sets within the range provided based on prior distribution, which was presented as the standard deviations calculated from parameter bounds (Doherty et al., 2015). Once the number of parameter sets are generated, the model is calibrated using all of them. It will result in the same number of calibrated models with different calibrated parameters (Herrera et al., 2022). Some calibrated models are rejected based on the preset performance criteria. For the rest, the results are ranked according to the probability of the capability of making predictions similar to observations, i.e., the best to least objective function (Herrera et al., 2022).

Chapter 3. Materials and Methods

3.1 Study area

The study site for the present study was station number 5 (49.62º N, -97.96 º W) of the 15 Real-Time In-situ Soil Monitoring for Agriculture (RISMA) stations installed by the Agriculture and Agri-Good Canada (AAFC) in 2011, 2013 and 2015 in Manitoba. Stations 1 to 9 are in the Carman-Elm Creek area (Figure 2.3) in the La Salle and Boyne River watersheds, part of the larger Red River basin (Pacheko et al., 2014). Stations 10-12 were installed in Sturgeon Creek Watershed in 2013, and the remaining were installed in 2015 at the Canada-Manitoba Crop Diversification Centre, northwest of Carberry, within the Assiniboine River basin. Station 5 is about 6.5 km southeast and 13.5 km northwest of Elm Creek junction and Carman. The site is characterized by a sub-humid climate, with average annual precipitation of 542.3 mm in the form of snow (146.1 mm) and rainfall (398.2 mm) based on the long-term historical climatic data from the Environment and Climate Change Canada website for the closest weather station (Elm Creek). The frost-free season lasts about 119 days to 126 days (Mills and Haluschak, 1993). The average annual temperature is 3.5ºC, with average maximum and minimum daily temperatures being 25ºC in July/August and below -20ºC in January, respectively.

The soil at the site is in the Vertisolic order within the suborder of Gleyed Humic Vertisol and Red River soils, respectively. Large and deep vertical cracks up to 80 cm in some parts of the area. The soil has imperfect internal drainage. The slope of the terrain is (0.5 to 2%) and undulating (Walker, 2012). The site occurs in the soil map unit named SCY5 – RIV (mixture of Scanterbury and Red River clayey soil) (https://agrimaps.gov.mb.ca/agrimaps/),). The textural percentages for the soil profile are presented in Table 3.1

Table 3.1 Textural classification of soil at the study site (Pacheko et al., 2014)

Depth (cm)	Sand (%)	SILT (%)	CLAY (%)	Textural class
5	41.4	18.1	40.5	Clay
20	22.7	19.5	57.8	Clay
50	4.3	27.2	68.5	Heavy Clay
100	3.0	27.7	69.3	Heavy Clay

3.2 Data collection

The soil water content, weather and crop data were collected to derive the data needed as input to the model. The growing season data was divided into two sets: the first was used for calibration, and the second was used to validate the calibrated parameters against the observed soil water content. For 2016 and 2018 (Soybean), calibration was performed for 80 days, and the parameters were validated for the rest of 50 days, whereas, for Oats, the division was 80 and 40 days, respectively.

3.2.1 Soil moisture data

Soil moisture sensors (Stevens Hydra Probes II) were installed in 2011 to monitor soil moisture continuously. Detailed descriptions of site preparation and the installation process are documented in Walker (2012). Soil moisture monitoring probes were replaced entirely in October 2014 following the malfunctioning of already installed sensors (Powers, 2014) and are being monitored continuously for data quality. These probes were installed within the cropped area, about 6-30 m inside of the edge of the field. Proper care is taken while seeding and harvesting around the site to protect the probes and improve the imitation of field conditions.

Additionally, re-installation of the top 2 sensors is done occasionally throughout spring and fall owing to rodents, cracking of the soil, and heaving. A total of 15 probes were installed to monitor soil moisture within the 0 - 5 cm and at 5 cm, 20 cm, 50 cm, and 100 cm. Three probes were installed per depth. The data from the top vertical probe installed within 0 – 5 cm is not accounted for in the study as the top layer is the most susceptible to soil's physical manipulation and environment. Soil moisture data obtained from the three probes installed at each depth during the growing seasons of 2016, 2017, 2018 and 2019 were averaged and used as the observed soil moisture for model calibration and validation in this study.

3.2.2 Crop data

Crop type and sowing date were obtained from Kurt (2023) as May 09, 2016 (Soybean), May 03, 2017 (Oats), May 10, 2018 (Soybean) and May 08, 2019 (Oats) and the harvesting dates were determined as September 15, August 30, September 16 and September 04 as most of the soybean varieties take 105-125 days and oats take about 90-110 days to mature according to Manitoba Agriculture and Seed Manitoba. Thus, harvesting was assumed to be done for soybeans and oats after 130 and 120 days, respectively. It also aligns with the average FAO guidelines for Soybeans. HYDRUS needs the crop root distribution as input to include the effect of crop water uptake. Less than 25% of the roots were assumed to grow beyond 0.20 m (Müller et al., 2021), as clay soil facilitates lateral root growth more than vertical, as the actual root distribution was unavailable.

3.2.3 Weather data

An on-site weather station is installed at the edge of the field that measures minimum and maximum temperature, average relative humidity, precipitation, wind direction and speed. The humidity and temperature data are measured at a height of 1.5 m using a Campbell Scientific temperature and relative humidity probe. Wind direction and speed are measured at 3 m and 2 m height, respectively, using an RM Young wind monitor. Precipitation is measured at the height of 1.5 m using Hydrological services TB4 tipping bucket rain gauge. The solar radiation data was taken from the Manitoba Agriculture station (roughly 25 km away), which was installed at Elm Creek. The pyranometers installed measure incident solar radiation in the last 24 hours. The collected data was used to calculate and interpret the data needed as input to the model for the parameter estimation process.

3.3 Simulation model

HYDRUS-1D, a widely used numerical model to simulate adequate water flow through the soil profile, was used with the single porosity model in this study. Richard's equation in Chapter 2 simulates the variably saturated flow, where the unsaturated hydraulic properties are described using van-Genuchten (1980) parameters. The model was provided with the following input settings and data.

3.3.1 Spatial and temporal resolution

The entire domain was divided into four layers: 0 –10, 10 – 30, 30 – 70 and 70 – 130 cm (Ojo, 2017). The whole domain (130 cm) was divided into 131 nodes to keep the resolution as fine as 1 cm to achieve an acceptable and stable numerical solution. The observation nodes were set at each point of probe installation, i.e., 5 cm, 20 cm, 50 cm, and 100 cm. The study only included the frost-free growing season from May to September. The daily variation of weather (effective precipitation, potential transpiration, potential evaporation) and soil water content instead of hourly was used to define the numerical solution, the upper atmospheric boundary condition data, printable output of simulated water contents, and the inverse solution.

3.3.2 Boundary conditions

The upper boundary condition was set to atmospheric with a surface layer to implement the effect of precipitation, evaporation, and land use. Implementing atmospheric boundary conditions requires precipitation, potential evaporation, transpiration, and a minimum value of pressure head allowed at the surface. The bottom boundary condition was set as free drainage. It is the most suitable boundary condition in the field to simulate a freely draining soil profile into the vadose zone (Šimůnek, 2013). Free drainage was assumed because the water table data was unavailable for the site.

3.3.3 Effective precipitation

Some part of precipitation is assumed never to reach the soil in agricultural cropped fields as the canopy may catch it. For the model input, effective precipitation was used instead of precipitation to account for the interception by the crop canopy during the growing season. Soybean canopy can intercept 15%-35% of total precipitation that is assumed never to reach the soil profile (Lull, 1964), while oats may intercept 21%-26% of rainfall (Baver, 1938). Equations 3.1 and 3.2 represent the interception amount and the precipitation reaching the ground, respectively, where LAI = Leaf Area Index.

$$\text{Interception rate} = \text{Maximum interception rate} \times \frac{\text{LAI}}{\text{maximum LAI}} \tag{3.1}$$

$$\text{Precipitation input} = \text{Measured precipitation} \times (1 - \text{Interception rate}) \tag{3.2}$$

3.3.4 Crop evapotranspiration

The FAO-Penman Monteith equation (Equation 3.1) is the standard equation to determine reference crop evapotranspiration (Allen, 1988).

$$E\,T_0 = \frac{0.408\Delta(R_n - G) + \gamma\frac{900}{T+273}u_2(e_s - e_a)}{\Delta + \gamma(1 + 0.34u_2)} \tag{3.3}$$

Where,

ET_0 = Reference Evapotranspiration

Δ = Slope of vapour pressure curve (kPa $^{0}C^{-1}$)

R_n = Net solar radiation at the crop surface (MJ m^{-2} day^{-1})

G = Soil heat flux density (MJ m^{-2} day^{-1})

γ = Psychrometric constant (kPa $^{0}C^{-1}$)

T = Mean daily air temperature at 2 m height (^{0}C)

e_s, e_a = Saturation, actual vapour pressure (kPa)

u_2 = Wind speed at 2 m height (ms^{-1})

The single time-averaged crop coefficient was used to calculate crop evapotranspiration from reference crop evapotranspiration (hypothetical grass).

$$ET_c = K_c * ET_0 \tag{3.4}$$

Kc was estimated using a graphical method. The detailed process is explained in Allen (1998). The process followed is briefly described here. The timelines for each stage were selected according to the FAO catalogue and Manitoba Agriculture guidelines. The values for $K_{c\ ini}$, $K_{c\ mid}$ and $K_{c\ end}$ for soybeans and oats were chosen from a table provided by Allen, 1998. Then, the coefficients were adjusted to local climatic conditions, followed by constructing the K_c curve as per the graphical method.

3.3.4.1 Partitioning of evaporation and transpiration

In HYDRUS, if the crop evapotranspiration is to be provided manually, it must be provided separately as potential transpiration and potential evaporation. The average LAI of Soybean was used as a coefficient to divide the potential crop evapotranspiration into potential transpiration and potential evaporation, which was calculated based on the Growing Degree Days (GDD) from equations 3.5 and 3.7 (Qiao, 2014; Setiyono et al., 2008). The maximum LAI for oats was assumed to be 5.5, as Coelho et al. (2019) reported the maximum LAI for oats from 4.06 to 8.13, and the LAI for each day was derived from curve fitting based on cumulative GDD.

$$\mathrm{LAI_{soybean}} = -0.000006(\mathrm{GDD_{cum}})^2 + 0.0124(\mathrm{GDD_{cum}}) \quad (3.5)$$

$$\mathrm{LAI_{oats}} = -0.000003(\mathrm{GDD_{cum}})^2 + 0.0081(\mathrm{GDD_{cum}}) \quad (3.6)$$

GDD_{cum} stands for the cumulative growth degree days (ºC) and can be expressed using the equation (Qiao 2014).

$$\mathrm{GDD_{cum}} = \sum_{i=1}^{n}[(\frac{\mathrm{T_{max}} - \mathrm{T_{min}}}{2}) - \mathrm{T_{base}}] \quad (3.7)$$

where,

T_{max} = maximum temperature of the day (ºC)

T_{min} = minimum temperature of the day (ºC)

T_{base} = base temperature needed for a crop to grow (Soybean=10ºC; Oats=5ºC)

Then, equations 3.8 and 3.9 were followed to estimate potential evaporation and transpiration.

$$\text{Potential Evaporation} = \mathrm{PET} \times e^{(-k \times \mathrm{LAI})} \quad (3.8)$$

$$\text{Potential Transpiration} = \mathrm{PET}\,[1 - e^{(-k \times \mathrm{LAI})}] \quad (3.9)$$

Where, k = coefficient governing radiation extinction by the canopy. (usually 0.5 – 0.75) (Šimůnek et al., 2009). In this study, k = 0.55 was used to represent that more than the upper half of the canopy contributed to surface heat and vapour transfer (Allen, 1998; Qiao, 2014).

3.4 Calibration model for parameter optimization

PEST (Parameter Estimation Software) is an external calibration tool that uses the Gauss-Marquardt-Levenberg method to receive the optimization (Doherty et al., 2004). A brief outline of the parameter estimation process and parameter set generation using HYDRUS and PEST is depicted in Table 3.2. It illustrates the process, and the software used to generate the text files. The input data derivation is described in 3.2.5.

Table 3.2 Software used to create files for parameter optimization

S. No.	Process	Software
1.	Create a project and a permanent directory to it.	HYDRUS GUI
2.	Setup geometry, layers, materials, main processes, upper and lower boundary conditions of the study domain.	HYDRUS GUI
3.	Assign initial soil hydraulic parameters for each layer of the domain.	HYDRUS GUI
4.	Setup time step control, nodal spacing, root distribution, initial conditions (soil water content).	HYDRUS GUI
5.	Export the input files in text format.	HYDRUS GUI
6.	Run the model through a window-based interface.	HYDRUS exe.
7.	Create a HYDRUS-PEST interface for parameter calibration.	Notepad ++
8.	Identify the parameters to be optimized. Create and check the PEST template file.	Notepad++, TEMPCHEK
9.	Identify the model-generated simulated values to be read by PEST for calibration. Create and check the PEST instruction file.	Notepad ++, INSCHEK
10.	Provide PEST with the name of the template, instructions, model input and output files, initial parameter values, ranges and control variables. Create and check the PEST input control file.	Notepad ++, PEST
11.	Run PEST and evaluate statistical parameters.	PEST
12.	Generate random sets of parameters and store them in different text files.	RANDPAR
13.	Create and execute a loop to run PEST with generated sets of parameters and store the obtained calibrated parameters and model outputs.	Notepad ++, PARREP, PEST
14.	Read the model outputs and statistical evaluation parameters for each optimization and sort the satisfactory model runs.	RDMULRES
15.	Calculate the probability of occurrence of each satisfactory parameter within a specific range.	Excel
16.	Final HYDRUS run using the most probable parameters as initial parameters.	HYDRUS 5.x

The upper and lower bounds were taken from the literature and adjusted according to the model convergence. Additionally, Gupta et al. (2021) reported that field-measured values for soil hydraulic conductivity were more significant than the laboratory-measured values, especially for soils with clay texture. Thus, the upper bound of K_s was set at a much higher value (10.20 m/day) for the topmost layer (0-10 cm) than the average values in the literature for clay soil.

3.4.1 HYDRUS-1D Inverse Modelling

Steps 1 to 5 were equivalently performed from Table 3.2 with the addition of inverse modelling process in step 2, and HYDRUS execution during this process was performed in the Graphical User Interface. The inverse modelling process needs inverse data information from observed conditions to define the objective function. The objective function (ϕ) measures the discrepancy between the simulated and observed data. Inverse modelling aims to minimize ϕ using the Levenberg-Marquardt nonlinear minimization method (Marquardt, 1963). Average volumetric soil water content observed with three sensors at each depth was provided to the model. The agreement between the modelled soil water content for each layer and the observed soil moisture from the probes installed at 5, 20, 50, and 100 cm was evaluated.

Along with the simulation results, it also produces a correlation matrix among the optimized parameters, which indicates the degree of correlation between the fitted parameters. It aids in selecting the parameters (if possible) to be fixed in estimation problems due to high correlation. The restriction to optimize a maximum of 15 parameters simultaneously poses a challenge, as user fixation of unknown parameters during the estimation process may result in misleading assessments. It eventually depends on the user to provide meaningful initial estimates and follow the process repeatedly until a global minimum is obtained. In the present study, 24 parameters (4 layers × 6 parameters) were to be optimized. Thus, hit and trial methods were used to fix different parameters.

3.4.2 PEST-HYDRUS Coupling

As there were 24 unknown parameters each year, it became a challenge as HYDRUS could optimize a maximum of 15 parameters at a time. Thus, PEST was used as a calibration tool. However, due to the high correlation among the parameters, θ_r and θ_s were fixed. This section briefly outlines how the HYDRUS-PEST couple was created and how it works. A thorough description of the model-PEST interface is provided by Doherty et al. (1995), and the same process was followed in this study. The method described in Table 3.2 was followed to create files to link executable HYDRUS and PEST. PEST needs three essential files to operate: Template, Instruction, and Input Control. Selector. It was used as a base to create the template file, as this is the file that introduces PEST to the parameters to be optimized. The instruction file was created based on the model output file that tells PEST about the output values to be read and compared with the measured initial values. These measured values are provided to PEST via an input control file.

Table 3.3 Settings used in PEST for parameter transformations

Parameter name	Trans-formation	Parameter change limit	Increment type	Increment	Derivative method
K_s	Log	Factor	Relative	0.01	Switch
α	None	Relative	Relative	0.01	Switch
n	None	Relative	Relative	0.01	Switch
l	None	Relative	Relative	0.01	Switch

This file also contains the names of template, instruction, model input and output file and model execution command. The calibration termination and parameter transformation criteria are also provided via this file. Thus, PEST repeatedly runs the model until either optimization is achieved or termination criteria are met. The optimized parameters, the correlation coefficient between simulated and observed values, the objective function and the number of models run in each optimization are recorded in a record (.rec) file written by PEST.

3.5 Repeated model runs and Model Refinement

Steps 12-15 were followed from the table to execute repeated model runs using 100 random parameter sets (Monte-Carlo sampling) to refine the calibrated model parameters. When generating each parameter value, the upper and lower bounds (range) were respected. As the calibrated parameters are sensitive to the initial parameter guess, 100 PEST input control files were created with the generated sets as the initial guess of parameters. A loop constructed in the batch file facilitated successive PEST-HYDRUS runs without user interference, and the process is illustrated in Figure 3.2.

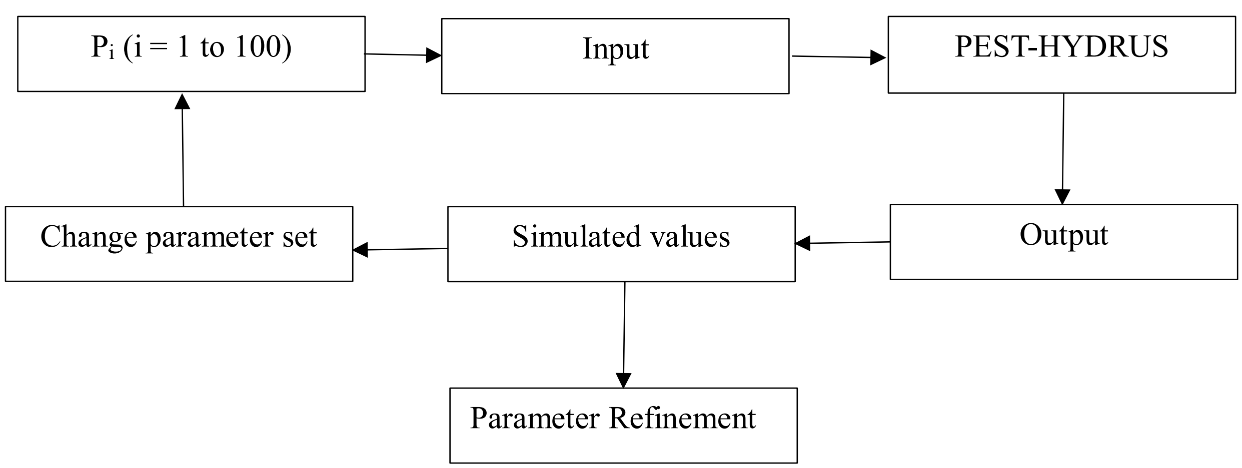

Figure 3.1 Flowchart explaining process of refining the calibrated parameter sets

After successfully running 100 optimizations, all the models were analyzed. Along with the correlation coefficient and objective function recorded in the pest output files, NSE, PBIAS, RMSE and R^2 were set as the model assessment parameters and are described in Chapter-2. The models were rejected due to these statistical parameters' unacceptable values and model convergence issues. The remaining calibrated model parameter sets were grouped into different bounds (narrowed range) followed by computing the probability of the parameter falling into each bound (for example, the initial range of K_s (0-10.20 m/day) for the top layer was subdivided into six intervals: 0-10, 10-30, 30-50, 50-70, 70-90, and 90-120). The parameter range with maximum likelihood in each category was then used as the final bounds for final parameter estimation.

Chapter 4. Results and Discussion

4.1 Weather conditions

The monthly rainfall received during the growing seasons (May-September) of 2016 to 2019 was compared to 20-year historical data (Figure 4.1a). The rainfall data was analyzed as the percent variation from normal data, where 100% suggests no variation. Total rainfall received during the 2016 and 2019 growing seasons did not have wide variation compared to the 20-year average (99.5% and 104%). Rainfall amounts varied differently among the months, as shown in Figure 4.1a. September was the driest month (37 mm) in 2016 and wettest (140 mm) in 2019. 2017 and 2018 were comparatively drier (about 62% each) against the long-term average. Rainfall amounts in 2018 were far less intense. For example, July and August received about 60 mm and 17 mm of rainfall, respectively. For the July event, 30 mm was received on July 11 within 45 minutes. For the August event, 15 mm was received on August 26 within 2 hours.

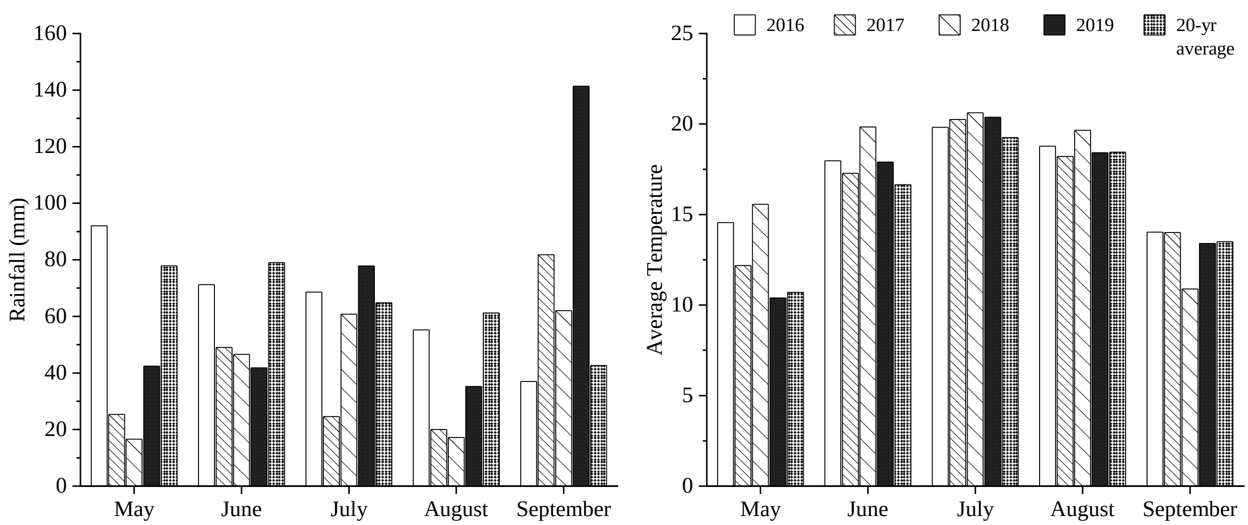

Figure 4.1 Comparison of (a) monthly total rainfall and (b) monthly average temperature during the study period and 20-yr long-term average

The monthly average temperature during the study period was compared to the average of at least 20 years (Figure 4.1b). June, July, and August were observed to be hotter compared to the historical average data. The average temperature for 2016, 2017, 2018, and 2019 were 16.38, 17.31, 16 .10, and 15.71 ^{o}C, respectively.

4.2 Soil water content distribution

4.2.1 Temporal soil water conditions

The soil volumetric water content measured at the 5 cm, 20 cm, 50 cm, and 100 cm depths and adequate precipitation reaching the ground surface after interception and the difference between the precipitation and potential crop evapotranspiration are presented in Figures 3.3 to 3.6. Rainfall events in 2016 were frequent and well-distributed as compared to other years. The common trend followed throughout the years was the increase in the water content of the top layer with weather conditions, as the water content changed proportionally to rainfall except for 2018. The increase in the water content after the rainfall was more than the decrease in soil moisture during the no-rainfall period (evapotranspiration only).

The water content at the bottom layers (50 cm and 100 cm) was always observed to be more than the top layers, except for May 28, following 68 mm of rainfall in the previous six days, when the water content at 5 cm reached saturation. The water content at 5 cm and 20 cm decreased when crop evapotranspiration was more significant than the rainfall. This reflects the contribution of these depths towards crop water use. The water content at 100 cm was near saturation for the whole study period, indicating the presence of an underlying slowly permeable layer that could have developed perched aquifer near the bottom boundary. It is common in Humic Glyesol soils to build an occasional perched water table (Manitoba Agriculture, 2010).

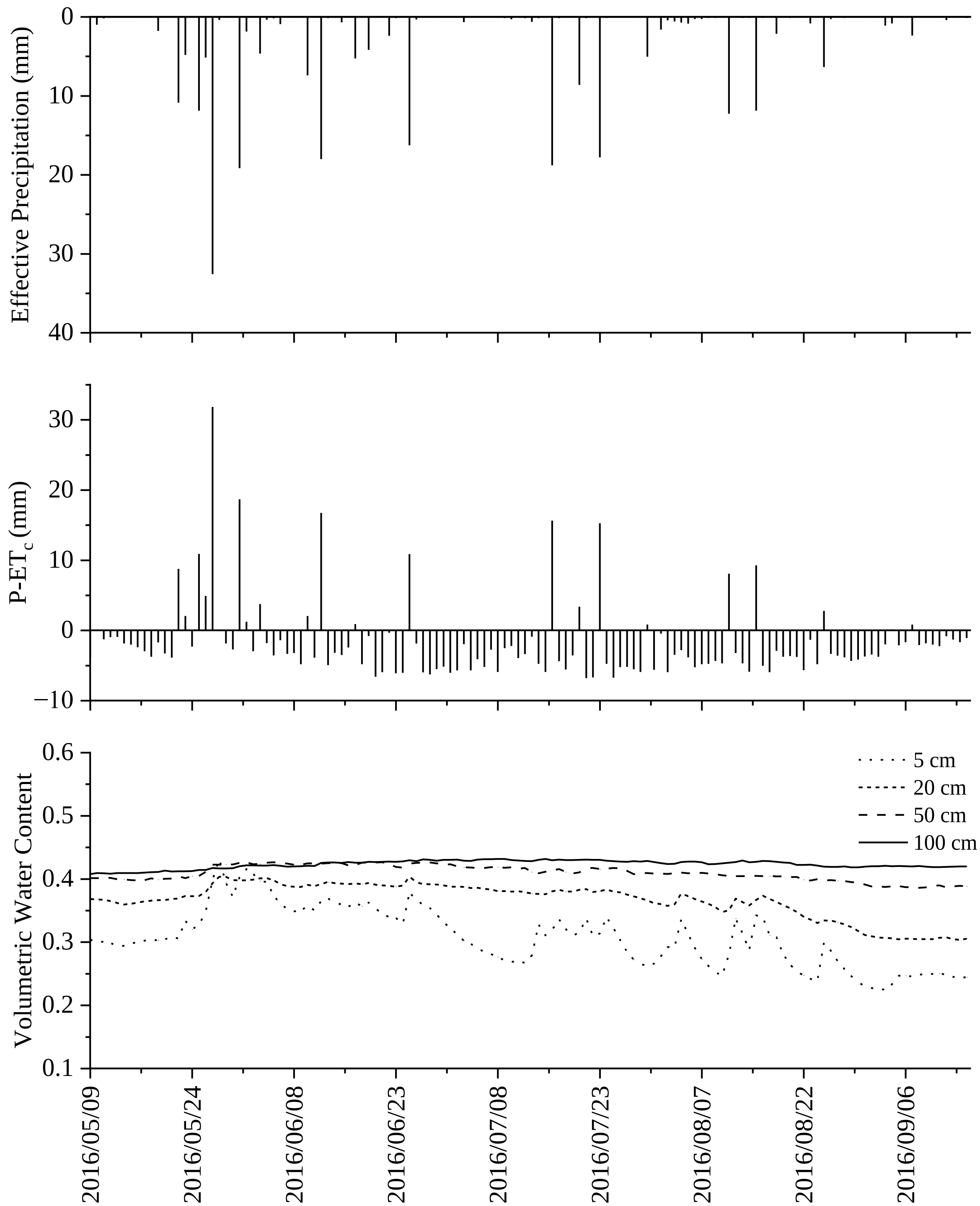

Figure 4.2 Temporal variation in soil water content with respect to effective precipitation and evapotranspiration for the 2016 study period

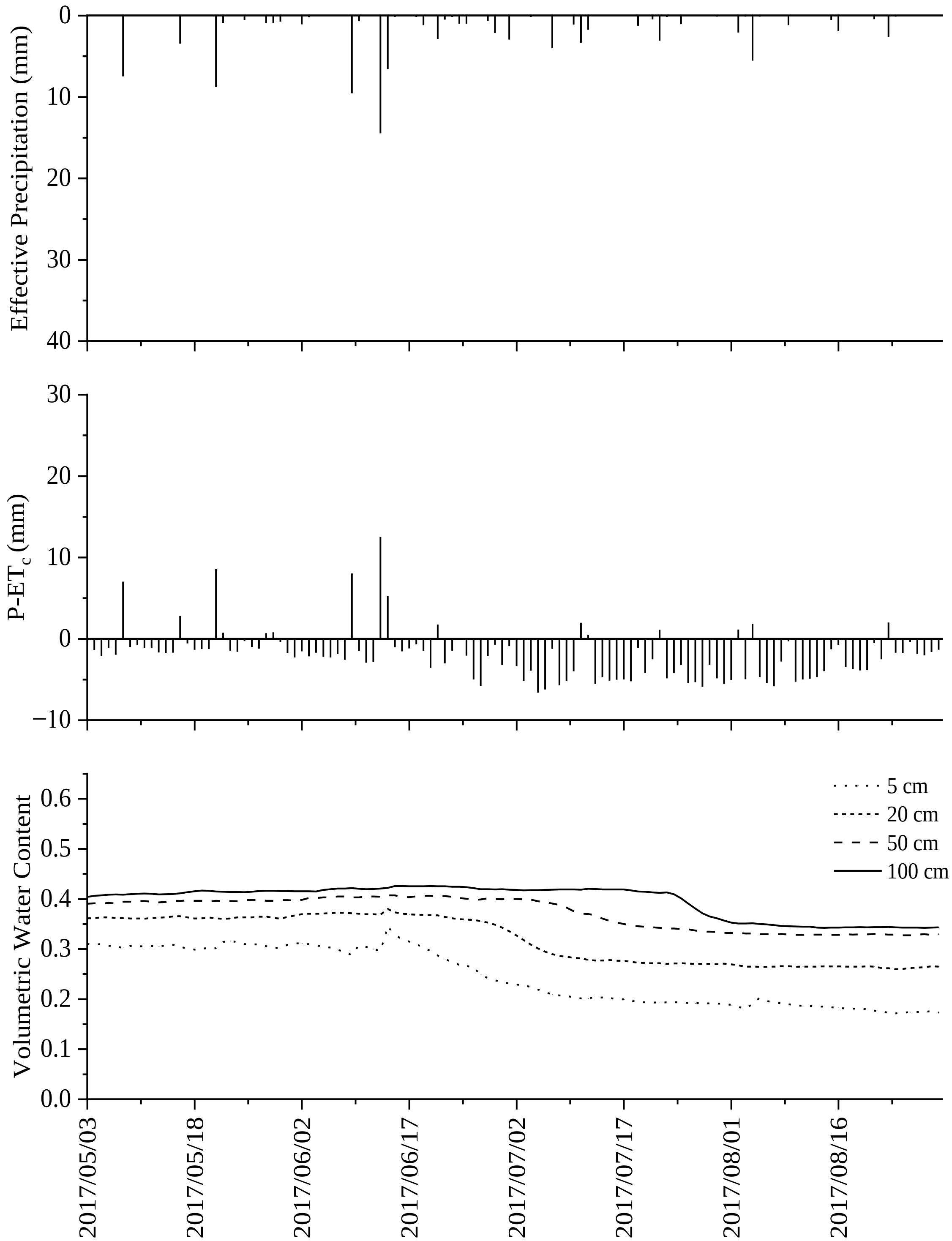

Figure 4.3 Temporal variation in soil water content with respect to effective precipitation and evapotranspiration for the 2017 study period

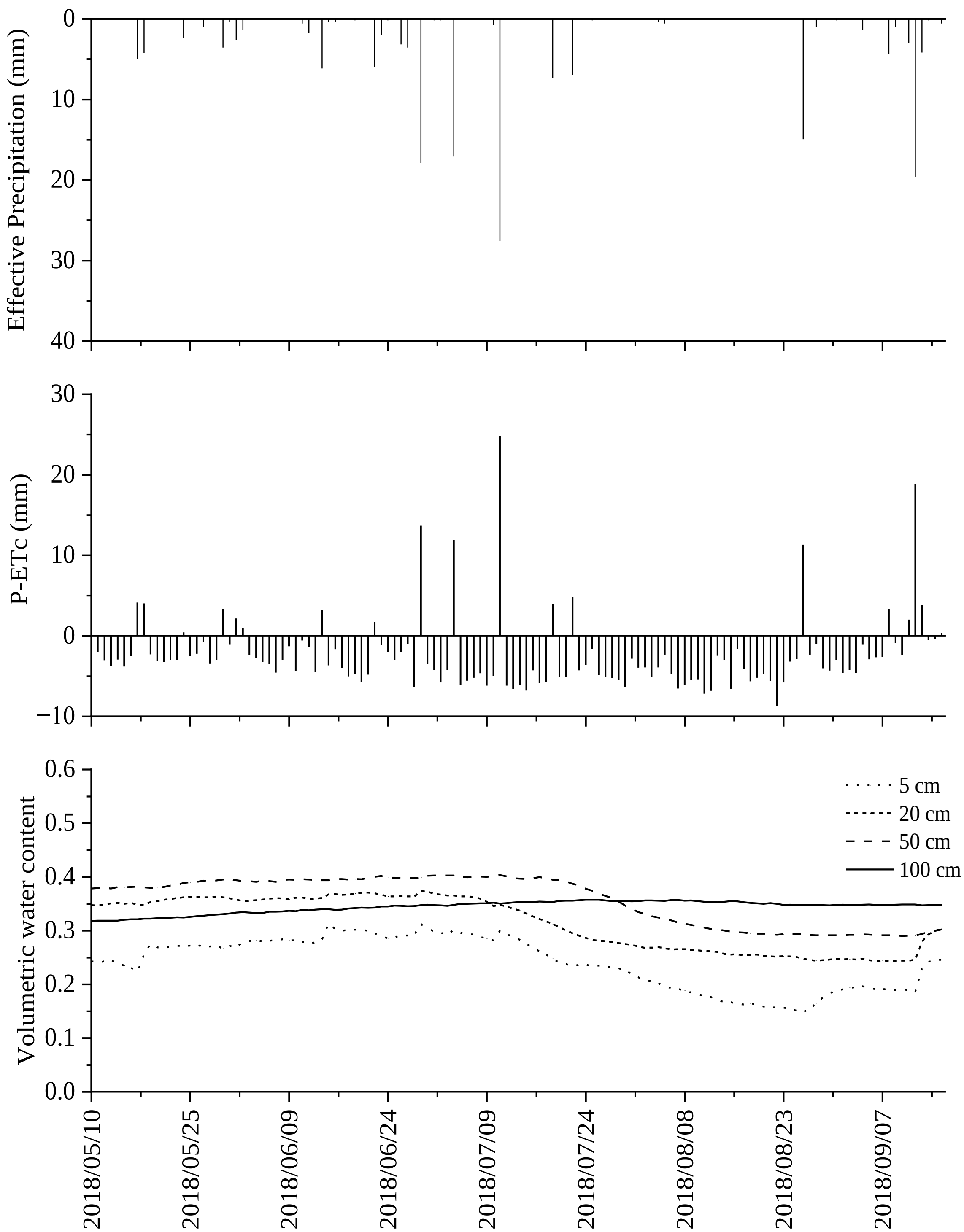

Figure 4.4 Temporal variation in soil water content with respect to effective precipitation and evapotranspiration for the 2018 study period

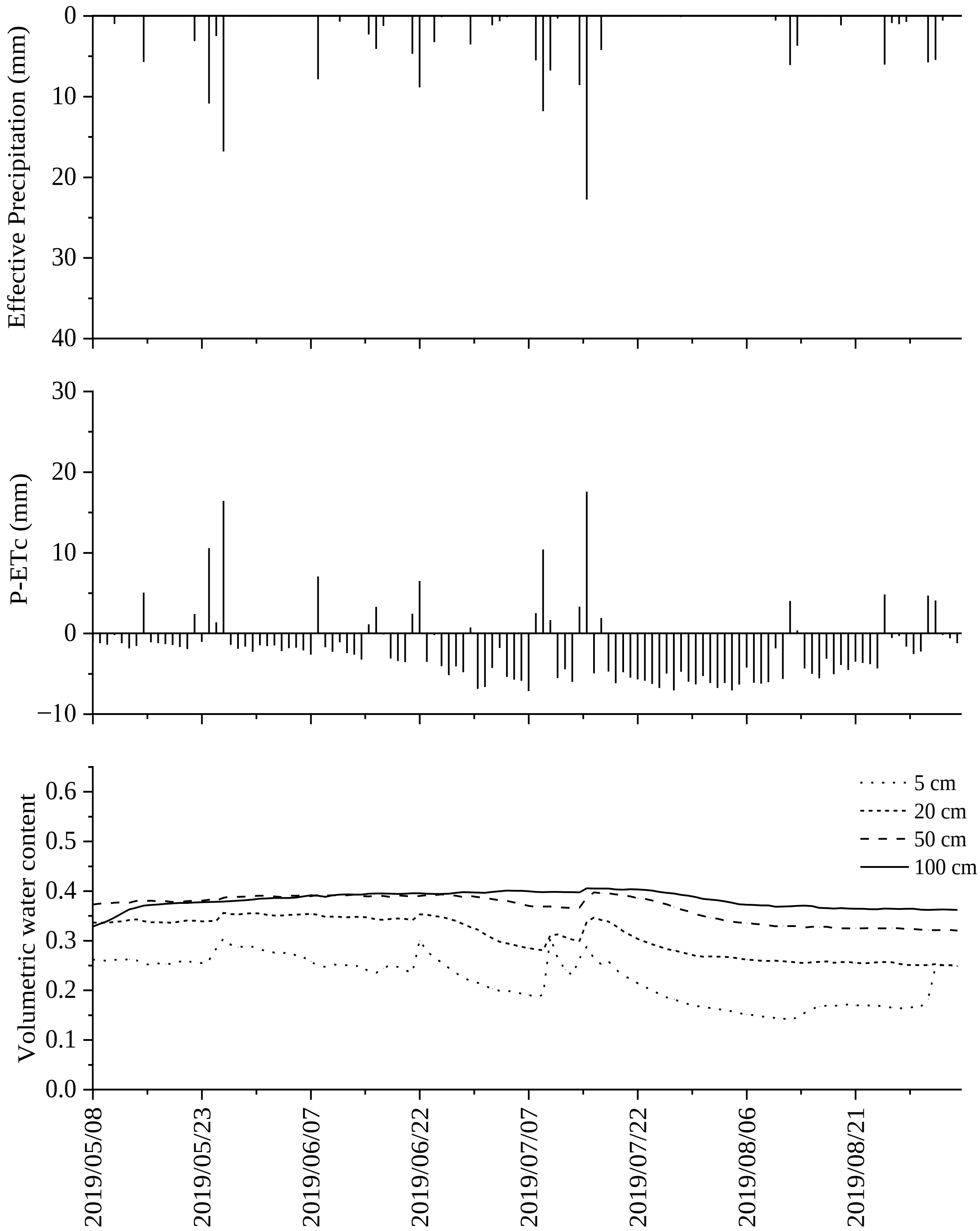

Figure 4.5 Temporal variation in soil water content with respect to effective precipitation and evapotranspiration for the 2019 study period

2017 had frequent rainfall events but received much less rainfall compared to evapotranspiration. The deeper the layers were, the higher water content was observed as the crop water uptake decreased with depth. A decrease in the soil water content for the whole profile was observed in July-August owing to less rainfall and the mid-season stage of crop when there is a high water requirement for evapotranspiration).

2018 showed a different soil water distribution compared to the other years. The moisture level at 100 cm was not affected. It was observed to be constant over the whole study period, demonstrating no soil moisture movement that further indicates either the presence of a capillary barrier between 50 cm and 100 cm or a slowly permeable layer underlying 100 cm that might have led to a perched aquifer. Also, less variation in the soil water content at 5 cm was observed following the rainfall event on July 11(27.4 mm in 1 hour during the night, of which 21.7 mm occurred in 15 minutes). There was almost no increase in the water content at 20 cm and 50 cm, which indicates the possibility of runoff with poor infiltration, as such high-intensity rainfall may cause surface crusting. In August, there was a rainfall event of 15 mm, which lasted for about 2 hours (distribution was no more than 3 mm of rainfall in 15 minutes), leading to slow infiltration and a gradual increase in moisture for the following 3 - 4 days.

Like other years, in 2019, the top layer was the most susceptible to weather conditions, and the drying occurred during the highest crop demand stage, with a corresponding decrease in moisture observed throughout the profile. The trends in the soil moisture for all the years also showed that the water content at 5 cm, 20 cm, and 50 cm decreased owing to the usage of water to meet the demand during the dry period (high crop evapotranspiration and less rainfall) from the end of July to end of August coinciding with a mid-season stage where the crop water requirement is the highest. This shows the contribution of moisture present in the profile towards crop water use.

4.3 Soil water distribution during the growth stages

The average water content during each crop growth stage was plotted against depth to examine the moisture dynamics during the various physiological stages of the crops (Figure 4.6).

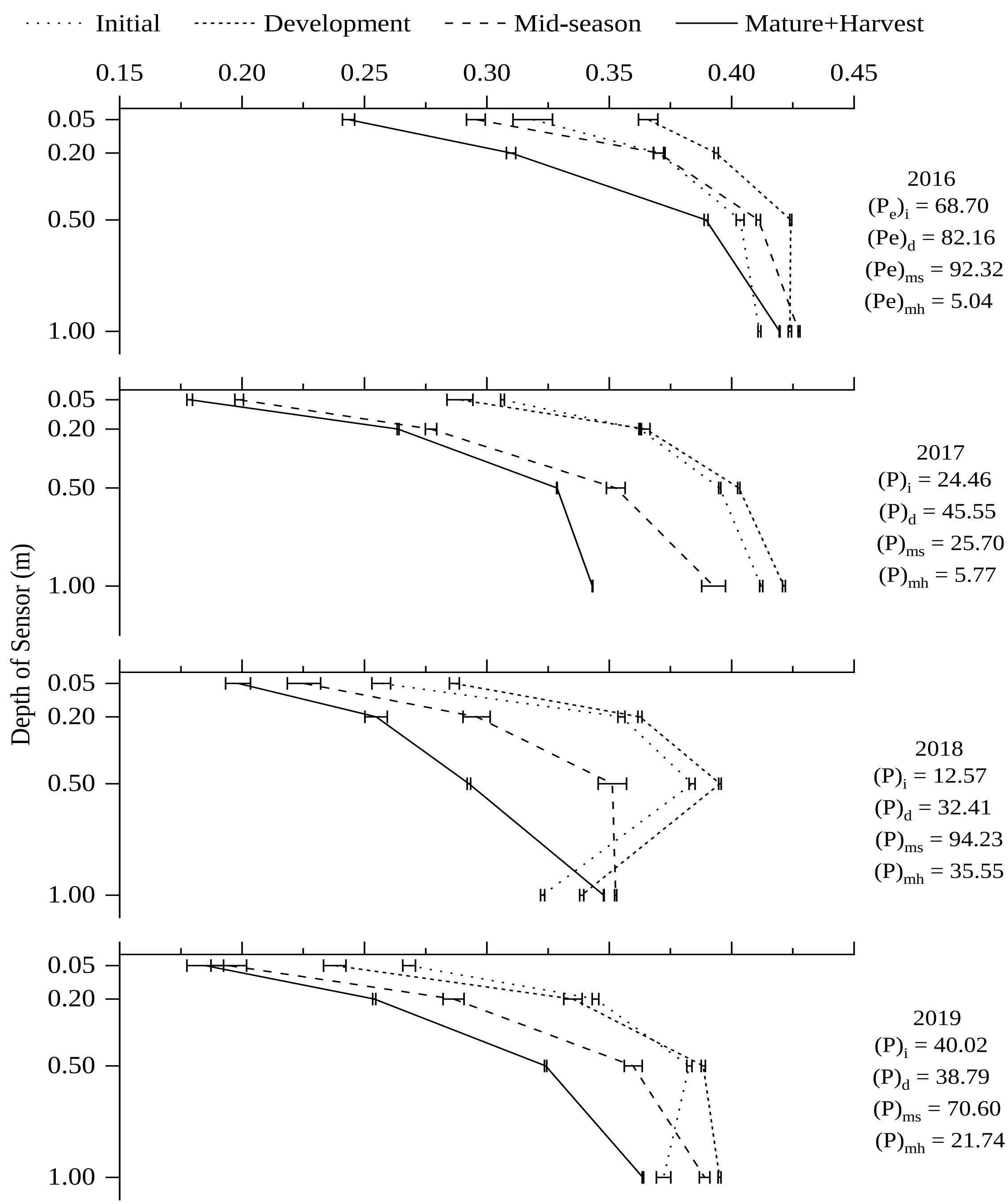

Figure 4.6 Soil water distribution during the growth stages

The stages were defined according to the FAO guidelines (Allen, 1998). The rainfall received was the lowest during the crops' last stages (mature + harvest) except for 2018. The average water content during the corresponding stage in all the layers was observed to be the lowest. For 2016, it was almost saturated for the whole period. 2018 showed a slightly different trend, where the 100 cm depth was wetter in the mature + harvest stage than in other stages, possibly due to the precipitation received during the mid-season stage. The water content at 5, 20, and 50 cm during the mid-season stage was always less than the initial and development stages despite having more precipitation because of high crop water uptake from these layers. This explains the dependence of moisture dynamics on the crop's physiological stages and the weather.

4.4 Initial Parameter Estimation

4.4.1 HYDRUS-1D Inverse Modelling and PEST+HYDRUS modelling

The initial estimation of the parameters from the HYDRUS inverse modelling and the coupled PEST and HYDRUS modelling for 2016 are presented in Table 4.1.

Table 4.1 van-Genuchten parameters estimated from HYDRUS and PEST+HYDRUS inverse modelling (2016)

Layer (cm)	HYDRUS Inverse Modelling					PEST + HYDRUS				
	θ_r	θ_s	α	n	K_s	θ_r	θ_s	α	n	K_s
0-10	0.17	0.45	0.0238	1.13	112.00	0.16	0.45	0.0196	1.13	119.30
10-30	0.28	0.41	0.0028	1.10	21.40	0.20	0.41	0.0040	1.05	44.73
30-70	0.21	0.44	0.0018	1.05	24.80	0.32	0.44	0.0004	1.14	6.32
70-130	0.33	0.44	0.0113	1.24	0.22	0.27	0.44	0.0117	1.05	0.11

It should be noted that the initial guess of parameters for the HYDRUS inverse modelling was selected from ROSETTA. In contrast, for the PEST-HYDRUS modelling, the initial estimate was the calibrated parameters from HYDRUS-1D inverse modelling.

4.4.2 Parameter non-uniqueness

Table 4.2 shows the model's performance based on the initial parameter estimation. As shown in Table 4.2, the model performance is acceptable for either approach used for parameter estimation. It can, however, be observed that optimized parameter sets are different from each other, which indicates the non-unique nature of the problem and the dependency of the calibrated parameters on the initial estimation. This questions the reliability of the parameters. This could be due to the high correlation among the parameters. High correlation among parameters results in different values of one parameter to another. The highest correlation between θ_r and K_s was 0.99, 0.98, 0.93, and 0.92 for the 0 – 10 cm, 10 – 30 cm, 30 – 70 cm, and 70 – 130 cm layers, respectively. High correlation is often observed in high-parametrized problems. Therefore, to reduce the number of optimizable parameters without prior information, manual regression was performed on only θ_s and θ_r by fixing their values based on the assumption that the soil has reached saturation at least once during the study period (Ojo, 2017). The value of θ_s was equal to the average maximum soil water content observed in 15-minute interval data for three probes located at 20, 50, and 100 cm depth for four years. As the probes located at 5 cm depth are re-inserted yearly, θ_s for the topmost layer were fixed as the maximum water content in that particular year.

A different approach was followed for residual water content, which can be below the permanent wilting point for fine-textured soils (Šimůnek, 2008). The value for θ_r was fixed using a Soil Hydraulic Properties Calculator developed by the University of Colorado. The water content equal to the lowest water content of the soil against infinitely high matric potential (-50000 m) by giving sand, silt, and clay percentages as input (Colorado State University, 2024) was set as θ_r. The values are presented in Table 4.6. as the residual and saturated water contents.

Table 4.2 Model evaluation results for estimated parameters presented in Table 4.1

Parameter	HYDRUS Inverse Modelling		PEST + HYDRUS		Acceptable values
	Calibrated	Validated	Calibrated	Validated	
NSE	0.87	0.74	0.88	0.67	0.00-1.00
PBIAS (%)	-0.30	-5.00	-1.10	-7.00	±10%
RSR	0.36	0.50	0.35	0.57	< 0.70
R-square	0.87	0.86	0.90	0.88	0.50-0.99

4.4.2.1 Repeated model calibration

Due to the sensitivity of calibrated parameters to the values of initial estimates in the model, inverse modelling was conducted using different initial forecasts. This process was automated with PEST, which repeatedly replaced the initial parameters in the control file after each calibration to receive a new set of calibrated parameters (repeated calibrations). As explained in the methodology section for 2016 to 2019, one hundred sets of initial parameter sets were generated, and calibration was performed for all these parameters. Results of 64, 21, 24, and 41 calibration runs were deemed satisfactory. These exclude the models resulting in the saturated hydraulic conductivity of the top layer (0-10 cm) lying below 10 cm/day to accept the practical solutions as the saturated hydraulic conductivity of disturbed silty to clayey agricultural soils is generally higher than 20 cm/day

(Kirkham, 2023). Only K_s was used as the criterion as it is sensitive to physical manipulation of the soil and weather variability.

The parameters optimized from the satisfactory calibrated models were then validated for the rest of the growing season by comparing the simulated water content with the observed water content (50 days for Soybeans and 40 days for Oats). Validation for each selected model for 2016, 2017, and 2019 was deemed satisfactory, except for 2018. To simplify the analysis, the parameters in each calibrated set for each layer were grouped within the narrowed intervals. Then, the number of sets falling into each range was counted along with the computation of average values and the maximum likelihood range. Figure 4.7 represents the probability distribution of the K_s parameter from 2016 to 2019 within the narrowed intervals. They reflect the parameters that fall into a specified group from all the satisfactory models to compute the maximum probable range. For example, the probability of K_s being optimized into the range of 10 - 30 cm/day is the ratio of models resulting in Ks value ranging from 10 - 30 cm/day to the total number of satisfactory calibrated models. The saturated hydraulic conductivity of the topmost layer was observed to be different over the years, and this variability was reduced with depth. The distribution showed different ranges for the second and third layers, but the maximum number of models gave the values in the same range over the years. Negligible variation was observed in K_s values optimized by different models

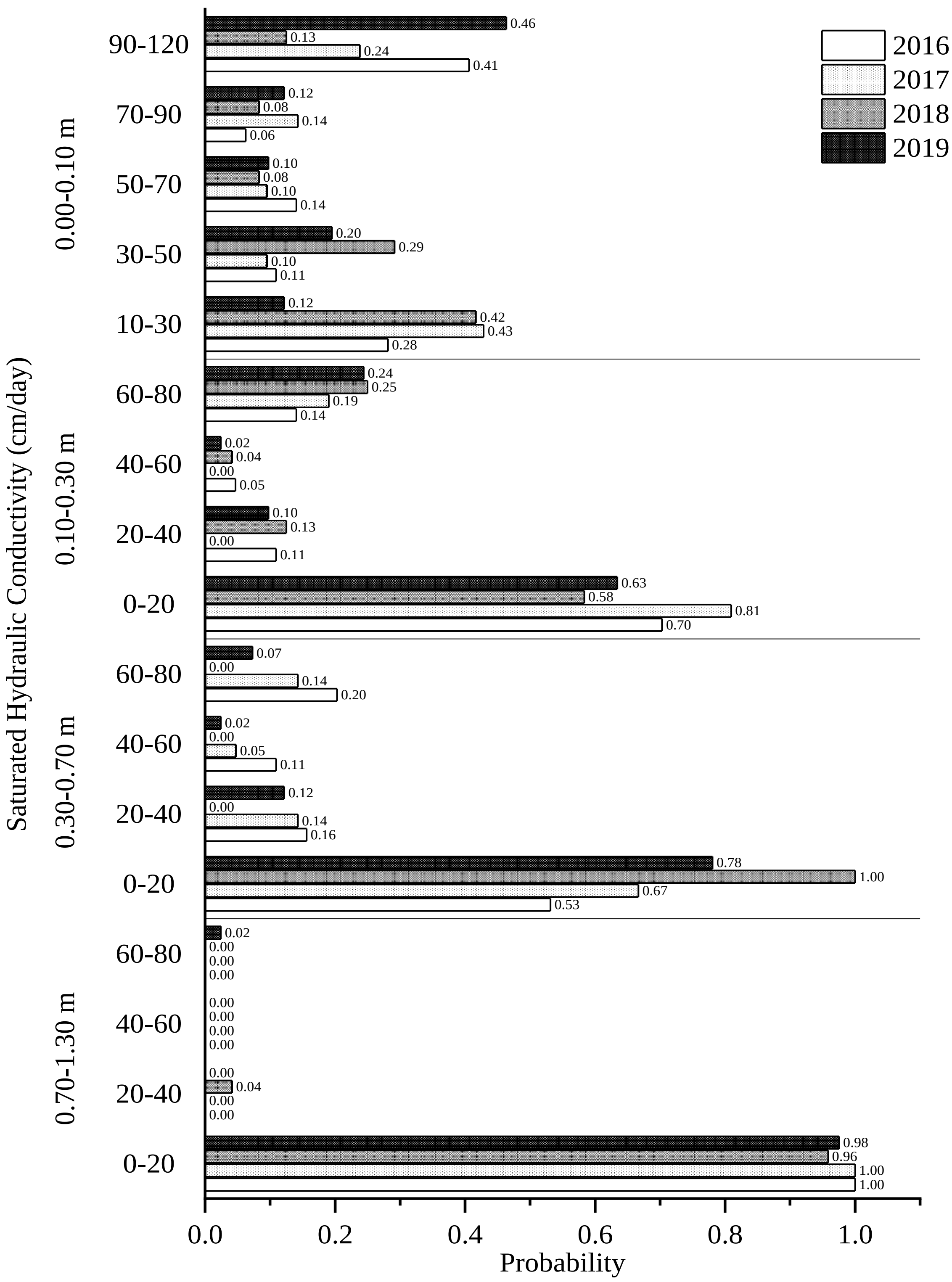

Figure 4.7 Probability distribution of K_s for 2016, 2017, 2018, and 2019 within narrowed intervals

4.5 Final Parameter Optimization based on most likelihood ranges

A final run for parameter estimation was done using a coupled PEST and HYDRUS model. The average of the parameters falling in the most probable range was used as the initial parameter set (Table 4.3 to Table 4.6). The parameter range with the highest probability was provided as the new narrowed upper and lower bound to the PEST control file for the final run for parameter estimation.

Table 4.3 Parameter control settings for the final parameter estimation run based on maximum likelihood range (2016)

Depth (cm)		θ_r	θ_s	α	η	K_s (cm/day)	*l*
0 - 10	Initial	0.10	0.43	0.0056	1.076	114.21	0.59
	Range	Fixed	fixed	0.001-0.01	1.05-1.15	90-120	0.58-0.60
	Final	**0.10**	**0.43**	**0.0021**	**1.11**	**120**	**0.58**
10 - 30	Initial	0.15	0.41	0.0007	1.05	5.10	0.52
	Range	fixed	fixed	0.0001-0.001	1.05-1.15	0-20	0.50-0.52
	Final	**0.15**	**0.41**	**0.0006**	**1.05**	**5.50**	**0.52**
30 - 70	Initial	0.20	0.42	0.0001	1.05	6.48	0.51
	Range	fixed	fixed	0.0001-0.001	1.05-1.15	0-20	0.50-0.52
	Final	**0.20**	**0.42**	**0.0001**	**1.06**	**6.09**	**0.50**
70 - 130	Initial	0.21	0.44	0.0002	1.05	0.39	0.52
	Range	fixed	fixed	0.0001-0.001	1.05-1.15	0-20	0.50-0.52
	Final	**0.21**	**0.44**	**0.0001**	**1.05**	**0.31**	**0.50**

Table 4.4 Parameter control settings for the final parameter estimation run based on maximum likelihood range (2017)

Depth (cm)		θ_r	θ_s	α	H	K_s (cm/day)	*l*
0 - 10	Initial	0.10	0.37	0.0038	1.19	19.97	0.59
	Range	fixed	fixed	0.001-0.01	1.15-1.25	10-30	0.58-0.60
	Final	**0.10**	**0.37**	**0.0163**	**1.15**	**10**	**0.58**
10 - 30	Initial	0.15	0.41	0.007	1.10	4.96	0.52
	Range	fixed	fixed	0.001-0.01	1.05-1.15	0-20	0.50-0.52
	Final	**0.15**	**0.41**	**0.01**	**1.14**	**3.65**	**0.52**
30 - 70	Initial	0.20	0.42	0.0033	1.07	7.441	0.50
	Range	fixed	fixed	0.001-0.01	1.05-1.15	0-20	0.50-0.52
	Final	**0.20**	**0.42**	**0.01**	**1.09**	**0.31**	**0.50**
70 - 130	Initial	0.21	0.44	0.0031	1.06	0.25	0.50
	Range	fixed	fixed	0.001-0.01	1.05-1.10	0-20	0.48-0.52
	Final	**0.21**	**0.44**	**0.001**	**1.11**	**0.43**	**0.48**

Table 4.5 Parameter control settings for the final parameter estimation run based on maximum likelihood range (2018)

Depth (cm)		θ_r	θ_s	α	H	K_s (cm/day)	l
0 - 10	Initial	0.10	0.36	0.0036	1.11	17.80	0.50
	Range	Fixed	fixed	0.001-0.01	1.05-1.15	10-30	0.50-0.52
	Final	**0.10**	**0.36**	**0.0091**	**1.07**	**21.21**	**0.50**
10 - 30	Initial	0.15	0.41	0.002	1.08	0.58	0.48
	Range	fixed	fixed	0.0001-0.01	1.05-1.15	0-20	0.48-0.50
	Final	**0.15**	**0.41**	**0.0031**	**1.05**	**0.26**	**0.50**
30 - 70	Initial	0.20	0.42	0.0002	1.08	1.73	0.52
	Range	fixed	fixed	0.0001-0.001	1.05-1.15	0-20	0.50-0.52
	Final	**0.20**	**0.42**	**0.001**	**1.05**	**0.80**	**0.52**
70 - 130	Initial	0.21	0.44	0.0002	1.06	0.39	0.51
	Range	fixed	fixed	0.0001-0.001	1.05-1.10	0-20	0.50-0.52
	Final	**0.21**	**0.44**	**0.0001**	**1.05**	**0.35**	**0.50**

Table 4.6 Parameter control settings for the final parameter estimation run based on maximum likelihood range (2019)

Depth (cm)		θ_r	θ_s	α	H	K_s (cm/day)	l
0 – 10	Initial	0.10	0.35	0.0337	1.29	114.24	0.59
	Range	Fixed	fixed	0.01-0.1	1.25-1.35	90-120	0.58-0.60
	Final	**0.10**	**0.35**	**0.1273**	**1.30**	**120**	**0.58**
10 - 30	Initial	0.15	0.41	0.0197	1.18	5.75	0.52
	Range	fixed	fixed	0.01-0.1	1.15-1.25	0-20	0.50-0.52
	Final	**0.15**	**0.41**	**0.0105**	**1.25**	**14.36**	**0.52**
30 - 70	Initial	0.20	0.42	0.0040	1.07	5.71	0.52
	Range	fixed	fixed	0.001-0.01	1.05-1.15	0-20	0.50-0.52
	Final	**0.20**	**0.42**	**0.0100**	**1.14**	**0.26**	**0.50**
70 - 30	Initial	0.21	0.44	0.0002	1.49	1.08	0.52
	Range	fixed	fixed	0.0001-0.001	1.35-1.50	0-20	0.50-0.52
	Final	**0.21**	**0.44**	**0.0001**	**1.44**	**0.01**	**0.52**

4.5.1 Model Evaluation

Figures 4.8 to 4.11 show the graphical representation of simulated and observed soil water content at 5 cm, 20 cm, 50 cm, and 100 cm for the final estimated parameters for 2016, 2017, 2018, and 2019.

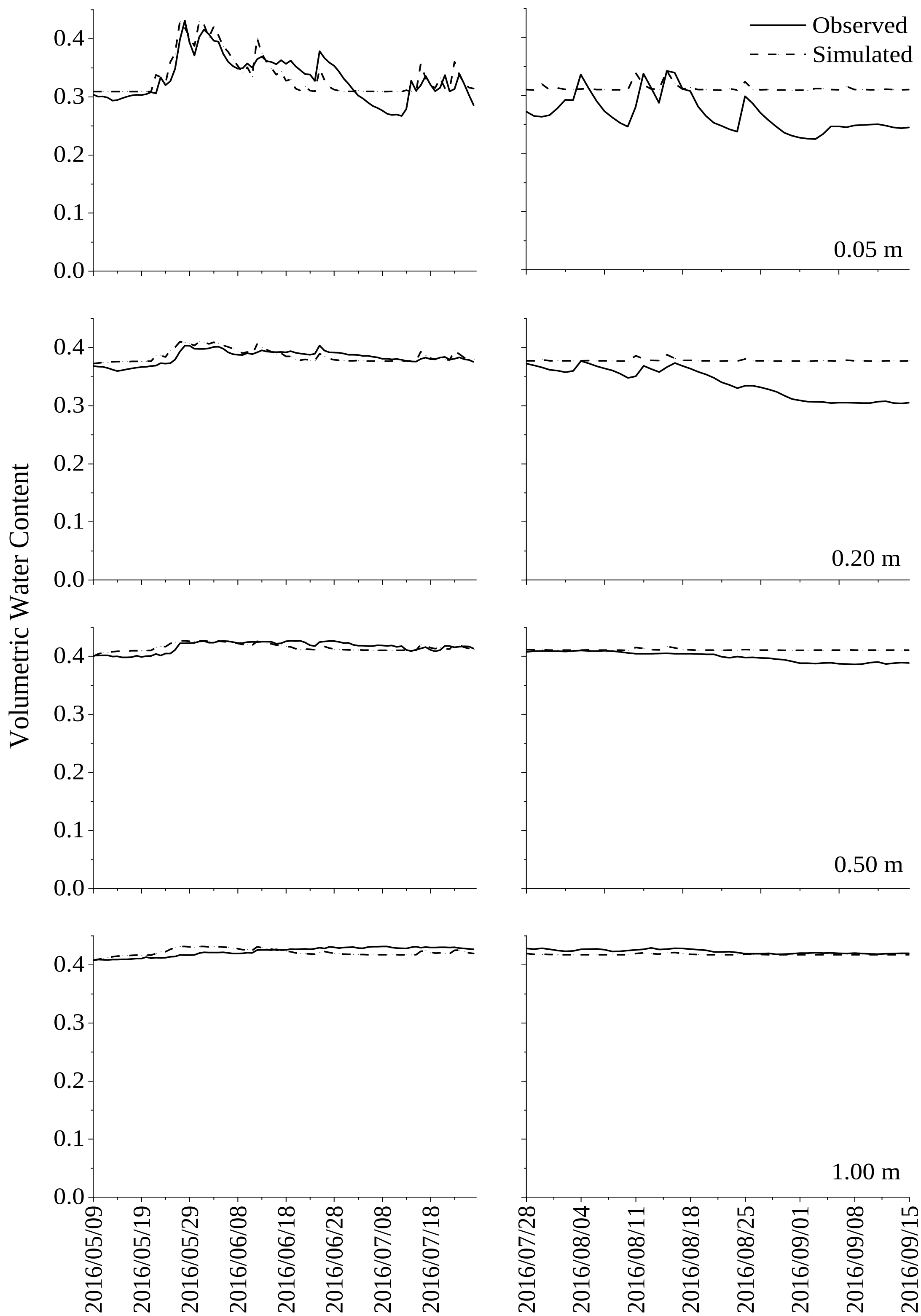

Figure 4.8 Visual comparison between observed and simulated volumetric soil water content for the 2016 study period

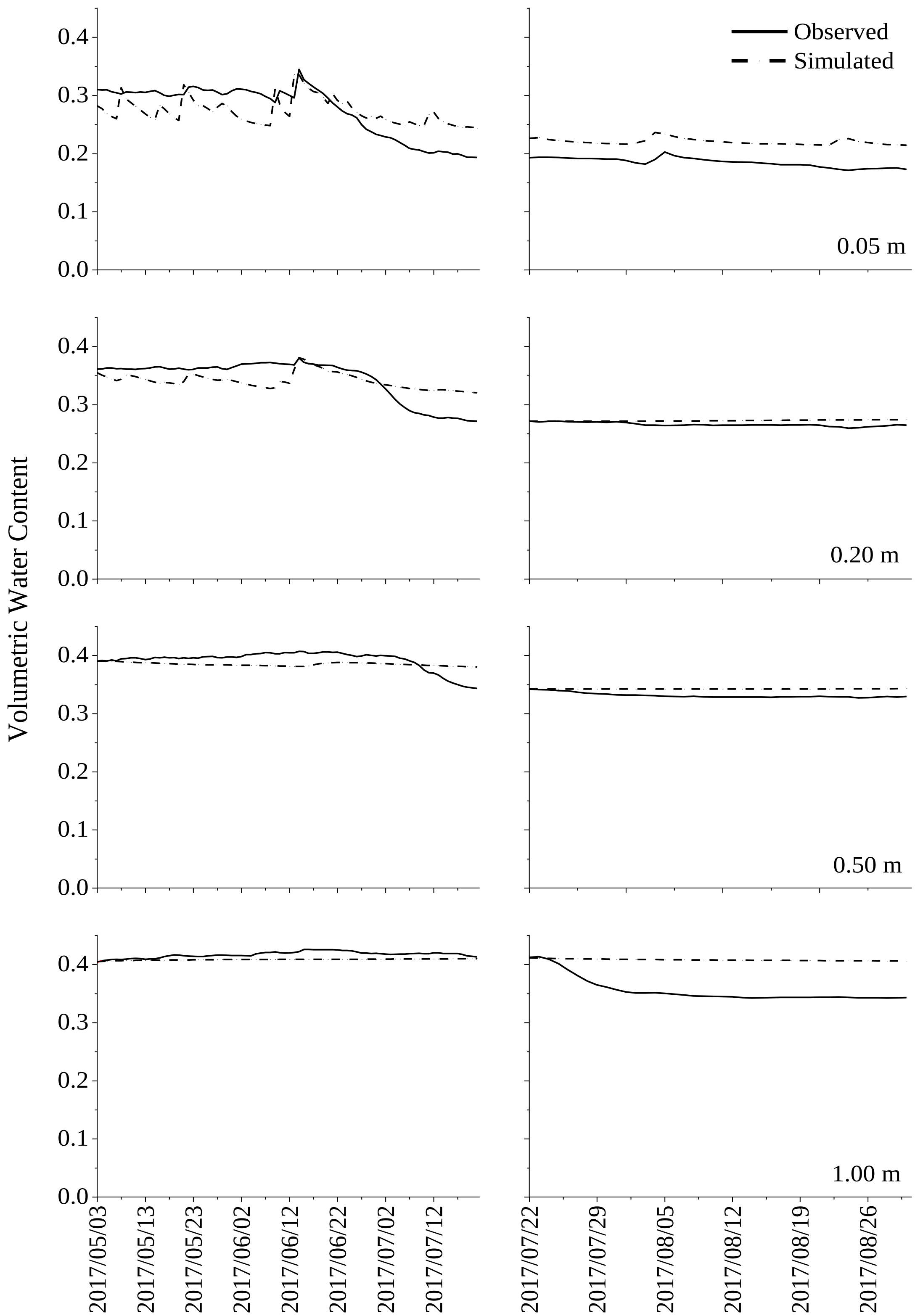

Figure 4.9 Visual comparison between observed and simulated volumetric soil water content for the 2017 study period

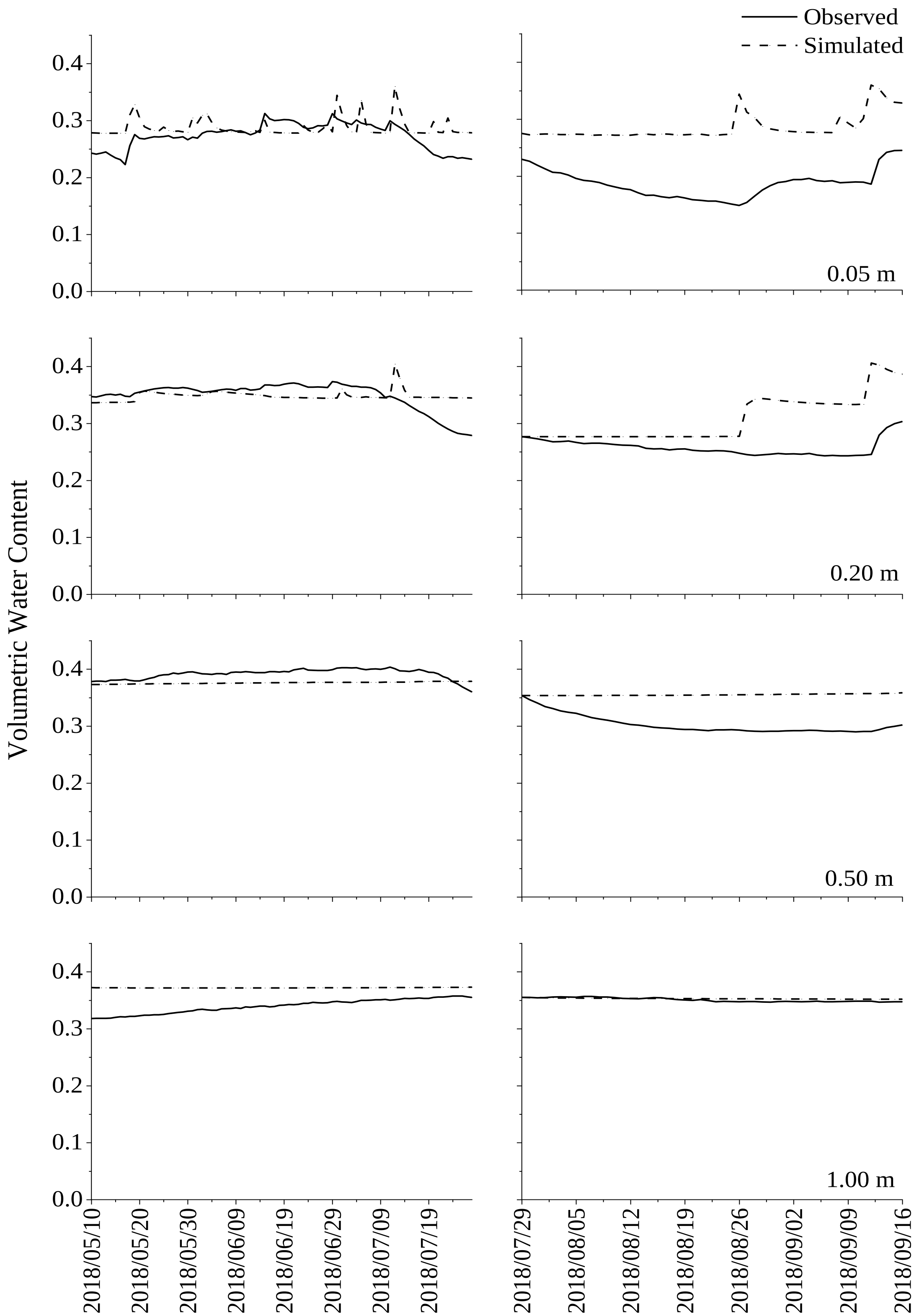

Figure 4.10 Visual comparison between observed and simulated volumetric soil water content for the 2018 study period

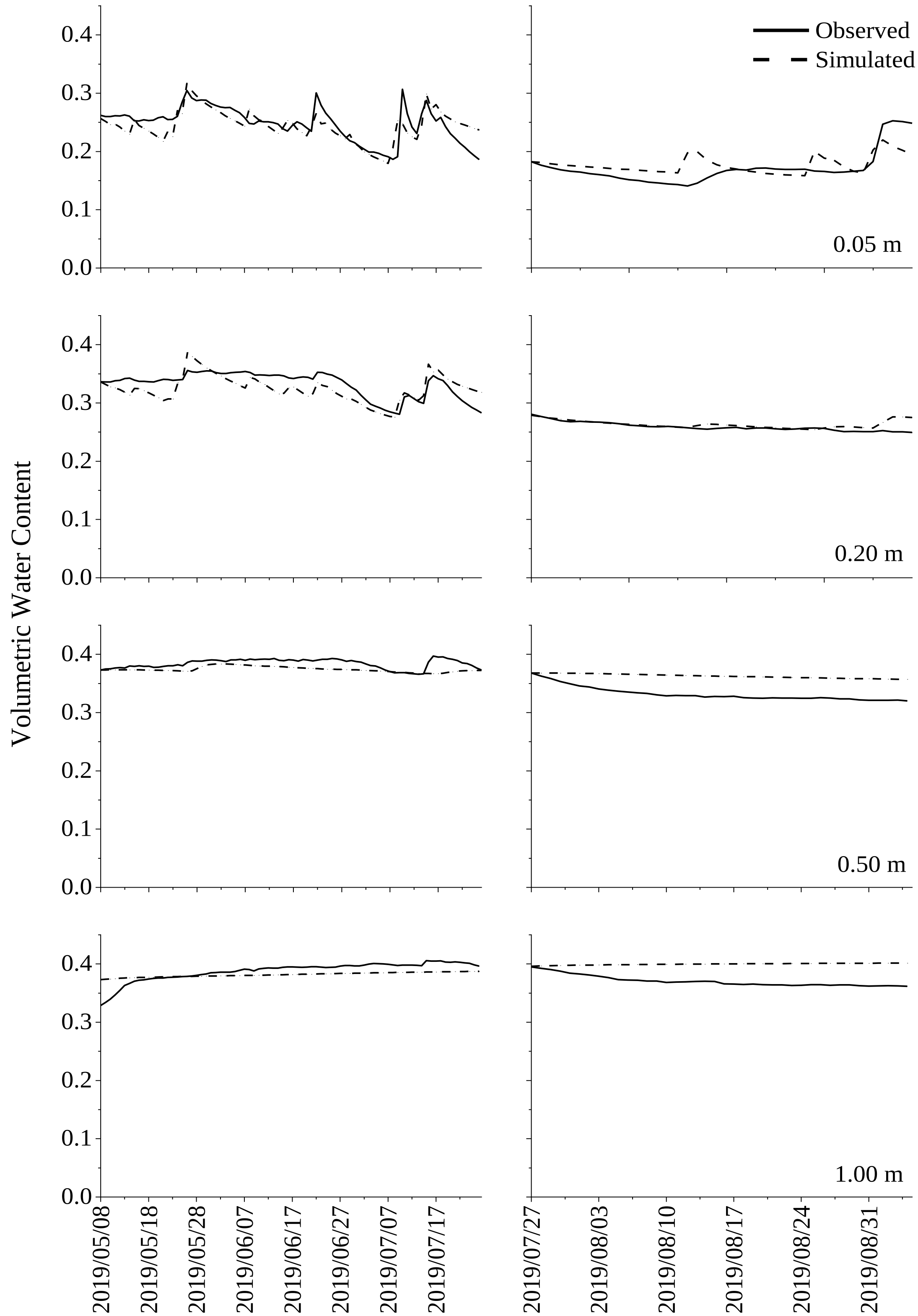

Figure 4.11 Visual comparison between observed and simulated volumetric soil water content for the 2019 study period

The trend followed by the simulated water content agreed with the observed water content except for the lowest water content observed in the top layers, which was observed in all the simulations for each year. The lowest observed water content was lower than the lowest simulated water content, which reflected the lowest water content below which the plant would not be able to extract water. This observation was attributed to the effect of Feddes parameters used in the model for root water uptake. The Feddes parameters were chosen for the crop with a drought tolerance similar to the HYDRUS catalogue. Using drought-tolerant varieties of crops can alter the Feddes' parameters. That is, the root system is slightly changed to bear dry conditions. For example, more root hair can pull water from the soils at higher matric potential than their sensitive counterparts during stressed periods (Rabbi, 2021). Also, stress-tolerant varieties do not necessarily decrease transpiration during droughts but can maintain the conductance of water from soil to roots through their enhanced root hair structure (Rabbi, 2021). A similar trend was observed for 2017 in the 0 – 10 cm and 10-30 cm layers. The agreement between the simulated and observed water contents in 2018 was good for calibration but poor for validation. This outcome was attributed to the response of the soil to weather variability.

In addition to the graphical representation of the simulated and observed soil water content, statistical parameters were used to evaluate the efficiency of the model to simulate the soil water content based on the final calibrated parameter set. As presented in Table 4.7, the model was deemed satisfactory for 2016, 2017, and 2019 during the calibration and validation periods. The model's performance for 2018 was satisfactory for the calibration period but poor for the validation period. The 2018 weather during the calibration stage may have given rise to significant shrinking and swelling of the soil. This effect alters the void ratio, which impacts the amount of water the soil can hold and the flow dynamics. The flow through shrink-swell soils cannot be well defined by assuming the single porosity model (Camporese et al., 2006; Stewart et al., 2016). Using a multi-domain (dual porosity) model is recommended to account for the changing void ratio and saturated hydraulic conductivities over time or divide the data into weekly or drying/wetting calibration and validation periods.

Table 4.7 Evaluation parameters calculated for final parameter estimation

Year		NSE	PBIAS	RSR	R^2
2016	Calibration	0.89	-0.28%	0.33	0.89
	Validation	0.68	-6.33%	0.57	0.88
2017	Calibration	0.84	1.48%	0.40	0.85
	Validation	0.74	-9.31%	0.51	0.91
2018	Calibration	0.65	-2.26%	0.59	0.68
	Validation	-1.13	-18.51%	1.46	0.01
2019	Calibration	0.92	1.99%	0.29	0.93
	Validation	0.89	-6.20%	0.33	0.96
	Accepted Values	0.0 -1.0	±10%	< 0.7	> 0.5

4.6 Comparison of simulations from initial and final calibrations

4.6.1 Graphical comparison among simulations

The water content simulated from 1) the HYDRUS-1D inverse modelling with initial estimates from ROSETTA, 2) calibration of HYDRUS-1D using PEST with initial estimates from HYDRUS-1D inverse modelling, and 3) final parameter optimization run using the initial estimates as an average of the values lying in the most likelihood ranges were compared graphically with the observed soil water content values for the entire study period (Figure 4.12). Simulations from all the approaches with the different sets of parameters reproduced the

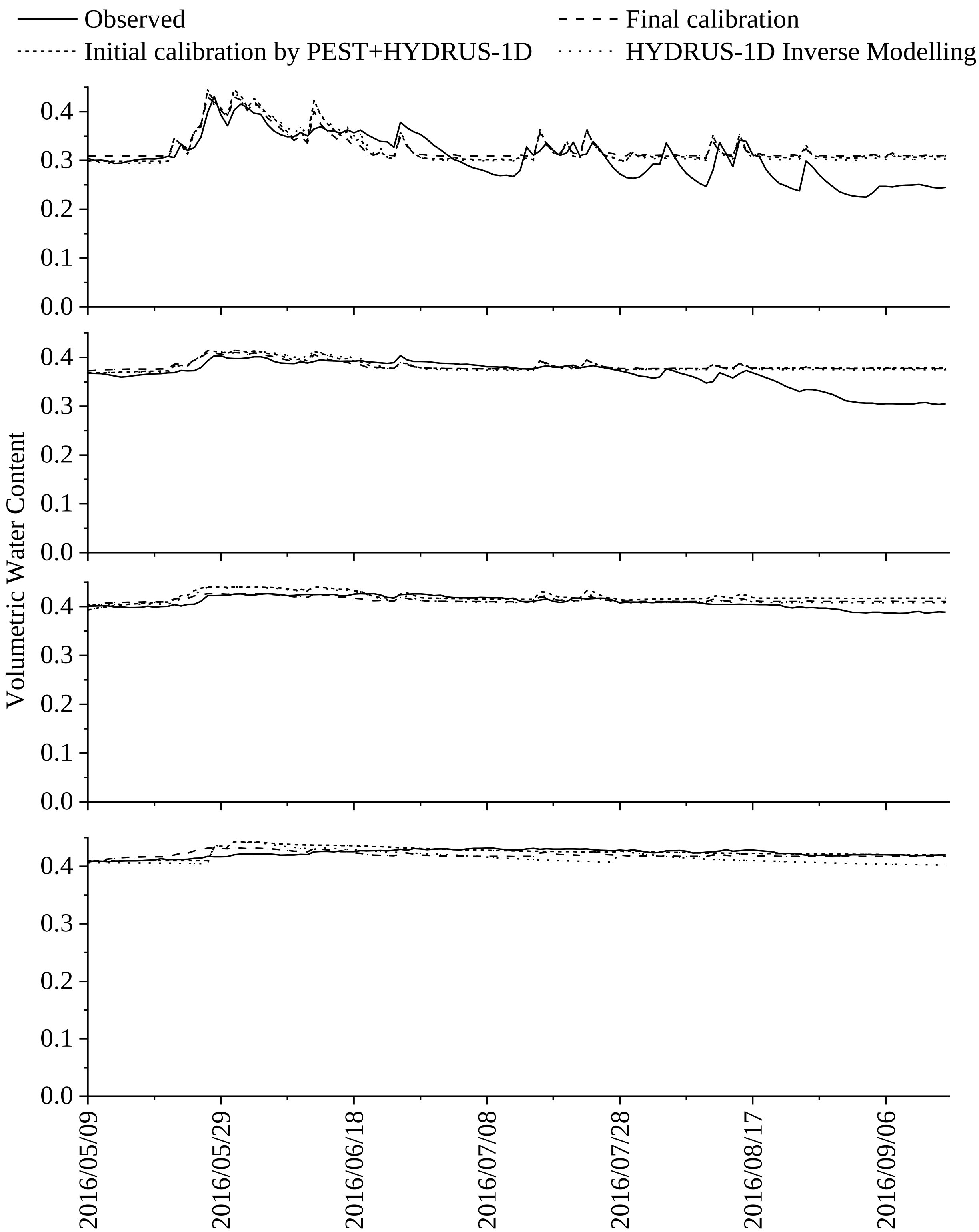

Figure 4.12 Graphical comparison of simulated soil water content with initial and final optimized parameters (2016).

observed data reasonably well. The agreement can be improved by using actual field data rather than assumptions. For example, the harvesting date of crops, crop type (drought tolerance of the crop), depth to the water table, and actual bottom boundary condition. It is recommended that rigorous uncertainty analysis be performed to better characterize the non-uniqueness of optimized parameters.

4.6.2 Mean comparison of simulated soil water content using the initial and final optimized parameter sets

A paired t-test was performed using JMP software (Version 18, SAS Institute, Inc, Cary, N.C) to compare 1) simulations from the finally calibrated parameters from the most likelihood ranges (Table 4.3) and the simulations from initial calibrated parameters from HYDRUS-1D inverse modelling (Table 4.1) for 2016 and 2) simulations from the finally calibrated parameters from the most likelihood ranges (table 4.3) and the simulations from initial calibrated parameters from coupled PEST + HYDRUS-1D (Table 4.1) for 2016.

The results (p-value) are summarized in Table 4.8. It was observed that the volumetric water contents simulated at 5 cm, 20 cm, and 50 cm using the calibrated soil hydraulic parameters during the final calibration run and initial HYDRUS-1D inverse modelling were not significantly different. The mean comparison of simulations from the initial calibration run using the coupled PEST+HYDRUS model and the final calibration run based on the maximum probable ranges were not significantly different for 5 cm and 20 cm. A significant difference was observed between the simulations using calibrated parameters from these two model runs at 50 cm.

Table 4.8 Statistical mean comparison of simulated soil water content with initial and final optimized parameters (2016).

Depth (cm)	Calibration	HYDRUS-1D Inverse Modelling (initial)	PEST+HYDRUS-1D (initial)
		p-value (α = 0.05)	
5	Final calibration run using most likelihood ranges	0.50	0.78
20		0.78	0.69
50		0.23	<0.0001
100		<0.0001	<0.0001

Meanwhile, the mean comparison of simulated soil water content at 100 cm was significantly different for all the approaches used for optimizing parameters. This observation was not apparent in the graphical representation (Figure 4.12). However, the mean comparison for the statistical parameters (NSE, PBIAS, and RSR) for the profile was not significantly different ($p = 0.99$).

4.7 Variation in Saturated Hydraulic Conductivity

Water flow dynamics in the soil profile define the effectiveness of soil water management strategies. (Isch et al., 2022). Hydraulic conductivity (saturated and unsaturated) is the most critical factor. The HYDRUS-1D model used in the study describes the unsaturated hydraulic function as the function of K_s and water content with empirical constants. This makes it critical to assess K_s and its evolution over time as it is sensitive to weather, soil and agronomic management practices. The saturated hydraulic conductivity of the top layer (plough horizon) is the most susceptible to physical manipulation and weather. Thus, the saturated hydraulic conductivity of each layer was compared over the years to explore its evolution under different cropping systems and weather characteristics (Figure 4.13).

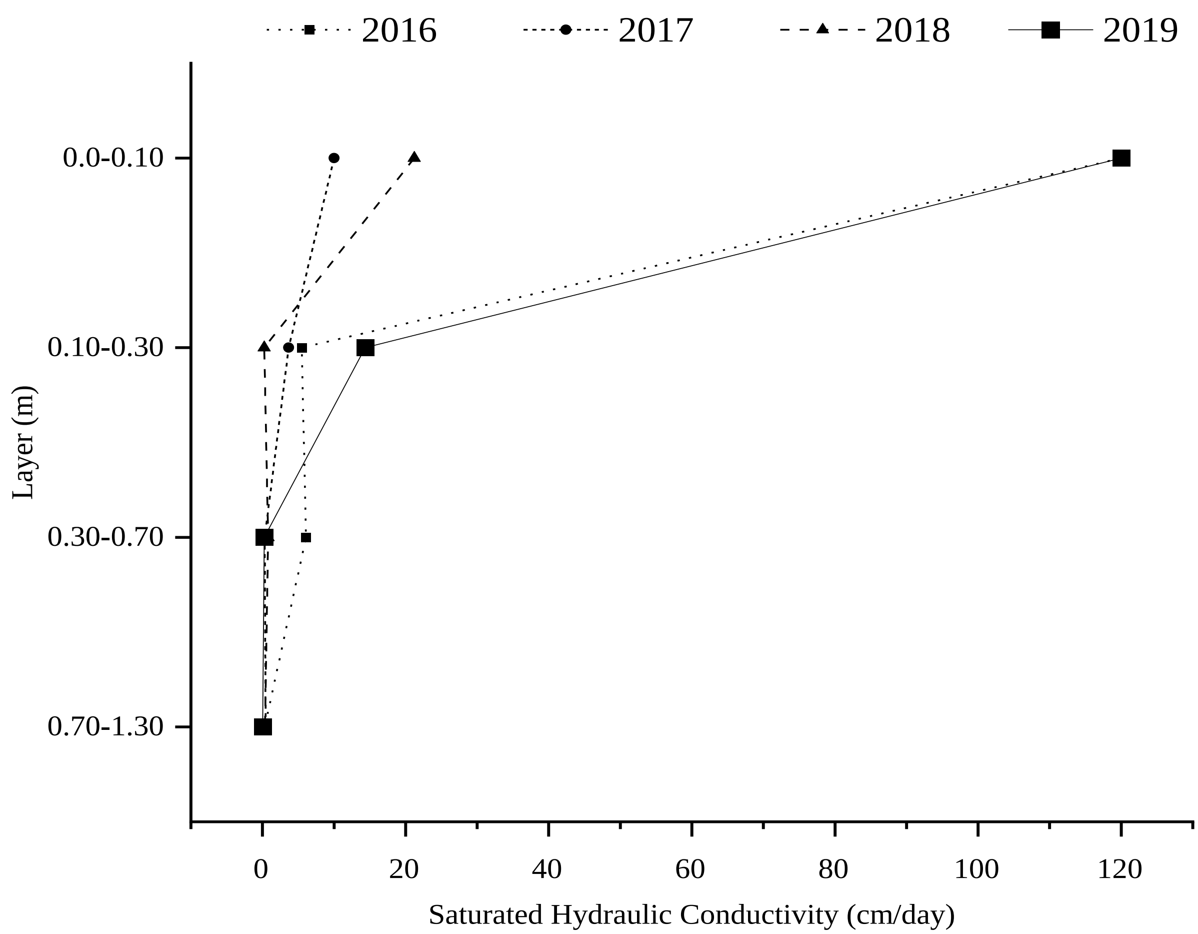

Figure 4.13 Variation of saturated hydraulic conductivity among years

The saturated hydraulic conductivity of 0.0-0.10 m layer was lower (10 cm/day) in 2017 and 2018 than in 2016 and 2019 (102.0 cm/day). The former years were comparatively drier than the latter. This demonstrates the dependency of K_s on weather and, hence, must be accounted for in determining strategies for soil water management. Low saturated hydraulic conductivity of 10 cm/day (2017) in the top layer will result in ponding for prolonged periods.

Chapter 5. Conclusions, Research Significance and Recommendations

5.1 Conclusions

The study estimated the van-Genuchten and Mualem soil hydraulic parameters for fine-textured soil in Manitoba using the inverse modelling approach within HYDRUS-1D and with an external calibration tool (PEST) coupled with HYDRUS. Both methods resulted in different parameter sets with acceptable values for statistical evaluation parameters. Repeated model calibrations were performed by generating 100 initial estimates of parameter sets. They repeatedly calibrated the model 100 times for each year, followed by computing the maximum likelihood of the parameter ranges. The most probable range and the average number of parameters in that range were provided to the model as the narrowed range and initial guess to run the final model calibration to estimate the parameters. The results from this study demonstrated that

- The solution to hydrologic scenarios is non-unique, and different parameter sets can perform similarly.
- PEST helped establish the non-linearity and non-unique nature of the solution.
- The model performance was satisfactory to excellent for 2016, 2017, and 2019 for the simulation of soil water content using the calibrated parameter sets. Poor model performance during 2018 validation shows that the physical manipulation of soil (tillage), physiological stage of the crop and soil response to weather (shrink-swell) can alter the soil hydraulic properties to a great extent within the season. Also, it reflects the natural hydrologic system exhibiting a non-linear nature with respect to the input variables. Calibrating a model under a forcing condition (weather) does not guarantee the same performance as predicting under different conditions. The saturated hydraulic conductivity varied over the years to the ratio of about ten times for the topsoil (plough horizon) but was almost constant for deeper soil layers.

5.2 Significance of Results

- The best objective function between the observed and the simulated conditions is often chosen to support and design a water management system. Different parameter sets resulted in a better value of one or the other statistical evaluation parameters, which can raise uncertainty and lead to poor decision-making. The probability distribution would help to choose the most likely parameter set for the solution. The results from this study suggest being cautious when selecting the parameter set that gives the best statistical values for decision-making if no prior information is available.
- Also, this study shows a close interaction between soil hydraulic properties management practices and weather conditions. It would help in the decision-making process for the physical operations on the field.
- The maximum likelihood parameter range determined in this study will serve as a database to support researchers in modelling soil structural and water dynamics for similar fields and boundary conditions.

5.3 Recommendations for Future Work

Based on the simulation process and the results, the following recommendations are made to improve model performance and the reliability of the simulation results:

- Use a dual-porosity model to account for the shrink-swell property as drastic weather change is a characteristics of the climate in Manitoba, or follow a different data treatment strategy to justify the changes in void ratio, pore connectivity factors, saturated hydraulic conductivity, bottleneck effects and the initial conditions followed by rigorous statistical analysis for better model performance.

- Identify calibration and validation periods to account for 1) changes in crop physiological stage that influence the rate of evapotranspiration and 2) wetting and drying cycles that impact the behaviour of shrink-swell soils. The physiological stages and the wetting and drying cycles alter the initial conditions specified in the model. Any drastic deviation from the specified initial condition can result in poor mode performance. This also suggests a relevant technique must be identified to integrate modelling and data analysis to simulate such a complex environmental system and compute uncertainty in the parameter estimation process.
- Determine water table depth (unconfined aquifer for heavy clay) to support the decision on choosing a bottom boundary condition for the site along with the crop variety and exact harvesting dates, as the model results depend on all these inputs.
- Studying at various locations in the same field would help develop spatiotemporal variations of these soil hydraulic parameters to better understand the overall soil water dynamics.

References

Abbaspour, K. C. (2022). The fallacy in the use of the “best-fit” solution in hydrologic modeling. *Science of the total environment*, *802*, 149713.

Abd Rashid, N. S., Askari, M., Tanaka, T., Simunek, J., and van Genuchten, M. T. (2015). Inverse estimation of soil hydraulic properties under oil palm trees. *Geoderma*, *241*, 306-312.Agriculture and Agri-Food Canada. (2023). Sustainable Canadian Agricultural Partnership.

Agriculture and Agri-Food Canada. (2024). Canadian Drought Monitor. Assessed: April 26, 2024.

Allen R. G., Pereira, L. S., Raes, D., and Smith, M. 1998. Crop evapotranspiration - Guidelines for computing crop water requirements - FAO Irrigation and drainage paper 56. FAO - Food and Agriculture Organization of the United Nations, Rome.

Anderson, M. P. and Woessner, W. W. (1991). Applied Groundwater Modeling, Simulation of Flow and Advective Transport. Academic Press, San Diego, CA, 381pp.

Asante, M., and Ashton, B. (2021). Downstream effects of Excess Moisture in Manitoba. April.

Asante, M., and Ashton, B. (2021). A Study Report of Economic Costs and Benefits Analysis of Proposed Investment Options for Farm-Level Extreme Moisture Management (Issue April).

ASCE. 1993. Criteria for evaluation of watershed models. J. Irrigation Drainage Eng. 119(3): 429-442.

Avissar, R. (1998). Which type of soil-vegetation-atmosphere transfer scheme is needed for general circulation models: A proposal for a higher-order scheme. J. Hydrol., 212–213, 136–154.

Babajimopoulos, C., Panoras, A., Arampatziz, G., Georgoussis, H., Hatzigiannakis, E. (2007). Contribution to irrigation from shallow water table under field conditions. Agricultural Water Management 92 (3), 205-210.

Baver, L.D. (1939), Ewald Wollny—A Pioneer in Soil and Water Conservation Research. Soil Science Society of America Journal, 3: 330-333.

Bekalu G. E., Hartmut M. H. (2019). Physical-Based Numerical Modelling to identify Permafrost Degradation due to Climate Change in Northern Manitoba

Bennett, N.D., Croke, B.F.W., Guariso, G., Guillaume, J.H.A., Hamilton, S.H., Jakeman, A.J., Marsili-Libelli, S., Newham, L.T.H., Norton, J.P., Perrin, C., Pierce, S.A., Robson, B., Seppelt, R., Voinov, A.A., Fath, B.D., Andreassian, V. (2013): Characterising performance of Environmental models. *Environ. Modell. Softw.* **40**, 1 – 20

Blair, D., Little, A., Wiens, M. (2010). Review of climate change projections for Southern Manitoba and potential impacts for agriculture. University of Winnipeg, AgriT-Environment Knowledge centre, Manitoba.

Borek, L.; Bogdal, A.; Kowalik, T. (2021). Use of Pedotransfer Functions in the Rosetta Model to determine Saturated Hydraulic Conductivity (K_s) of Arable Soils: A Case Study. Land, 10, 959.

Brooks, R. H., and Corey, A. T. (1964). Hydraulic properties of porous media, *Hydrol. Paper No. 3*, Colorado State University, Fort Collins, CO.

Brunetti, C., Bianchi, M., Pirot, G., and Linde, N. (2019). Hydrogeological model selection among complex spatial priors. *Water Resources Research*, *55*(8), 6729-6753.

Camporese, M., Ferraris, S., Putti, M., Salandin, P., and Teatini, P. (2006), Hydrological modeling in swelling/shrinking peat soils, Water Resour. Res., 42, W06420, doi:10.1029/2005WR004495.

Carsel, R. F., and Parrish, R. S. (1988). Developing joint probability distributions of soil water retention characteristics. *Water resources research*, *24*(5), 755-769.

Cherif, E., Feilhauer, H., Berger, K., Dao, P. D., Ewald, M., Hank, T. B., He, Y., Kovach, K. R., Lu, B., Townsend, P. A., and Kattenborn, T.: From spectra to plant functional traits: Transferable multi-trait models from heterogeneous and sparse data, Remote Sens. Environ., 292, 113580.

Christianson, L.E., J. Frankenberger, C. Hay, M. J. Helmers and G. Sands, 2016. Ten ways to reduce nitrogen loads from drained cropland in the Midwest. Pub. C1400. University of Illinois Extension.

Climate Change Connection. (2013). Farming in a Changing Climate in Manitoba. A guide to sustainable cropping systems - April 2023.

Coelho, A.P., Faria, R.T.de., Barbosa, A.M. da S., Dalri, A.B., Rosalen, D.L. (2019). Performance of white oats cultivated under fertigation with treated sewage effluent and definition of critical limits of normalized difference vegetation index. Bragantia, 78(4), 553-563.

Colorado State University. (2024). Soil Hydraulic Properties Calculator. Date assessed: May 19, 2024. https://biocycle.atmos.colostate.edu/shiny/soils

Cordeiro M.R.C. (2014). Agronomic and Environmental Impacts of Corn Production under Different Water Management Strategies in the Canadian Prairies. PhD. Thesis. University of Manitoba, Canada

Diminescu, M. A., Dumitran, G. E., and Vuţă, L. I. (2019). Experimental methods to determine the hydraulic conductivity. E3S Web of Conferences, 85, 1–7.

Doherty, J., Brebber, L., Whyte, P. (1995). PEST. Model Independent Parameter Estimation. Australian Centre for Tropical Freshwater Research: James Cooke University, Townsville, Australia.

Doherty, J., 2010a, PEST, Model-independent parameter estimation—User manual (5th ed., with slight additions): Brisbane, Australia, Watermark Numerical Computing.

Doherty, J., 2010b, Addendum to the PEST manual: Brisbane, Australia, Watermark Numerical Computing.

Doherty, J., 2015. Calibration and Uncertainty Analysis for Complex Environmental Models. Watermark Numerical Computing, Brisbane, Australia. ISBN: 978-0-9943786-0-6

Doherty, J.E., Hunt, R.J., and Tonkin, M.J. (2010) Approaches to highly parameterized inversion: A guide to using PEST for model-parameter and predictive-uncertainty analysis: U.S. Geological Survey Scientific Investigations Report 2010–5211, 71 p.

Durner, W. (1994). Hydraulic conductivity estimation for soils with heterogeneous pore structure, *Water Resour. Res.*, *32*(9), 211-223.

Eden, M. R., Siirola, J. D., and Towler, G. (2014). *Proceedings of the 8th International Conference on Foundations of Computer-Aided Process Design*. Elsevier.

Eslamian, S., Sayahi, M., Ostad-Ali-Askari, K., Basirat, S., Ghane, M., Matouq, M. (2018), Saturation: Encyclopedia of Engineering Geology. Encyclopedia of Earth Sciences Series. 10.1007/978-3-319-12127-7_251-1

Feng G.L. et al., (2003). Evaluation of a model for irrigation management under saline conditions: 1. Effect on plant growth Soil Sci. Soc.Am. J., 67 (2003), pp. 71-76

Franzen, D., Augustin, C., DeSutter. T., Kalwar, N. (2024). Managing saline soils in North Dakota.

Geo-Slope International Ltd. (2015). Seepage Modelling with SEEP/W. Engineering Methodology. June 2015 Edition.

Gupta, S., Lehmann, P., Bonetti, S., Papritz, A., and Or, D. (2021). Global prediction of soil saturated hydraulic conductivity using random forest in a Covariate-based GeoTransfer Function (CoGTF) framework. Journal of Advances in Modeling Earth Systems, 13, e2020MS002242.

Guzman, J.A.; Shirmohammadi, A.; Sadeghi, A.M.; Wang, X.; Chu, M.L.; Jha, M.K.; Parajuli, P.B.; Harmel, D.R.; Khare, Y.P.; Hernandez, J.E. (2015). Uncertainty considerations in calibration and validation of hydrologic and water quality models. Transactions of the ASABE, 58(6), 1745–1762.

Harmel, R.D., P.K. Smith, K.W. Migliaccio, I. Chaubey, K.R. Douglas-Mankin, B. Benham, S. Shukla, R. Muñoz-Carpena and B.J. Robson, B. J. (2014). Evaluating, interpreting, and communicating performance of hydrologic/water quality models considering intended use: A review and recommendations. Environmental Modelling and Software 57: 40–51.

Herrera, P.A., Marazuela, M.A., Hofmann, T. (2022). Parameter estimation and uncertainty analysis in hydrological modelling. Wiley Interdisciplinary Reviews: Water, 9(1), e1569.

Hopmans, J. W., Šimůnek, J., Romano, N., and Durner, W. (2002). 3.6. 2. Inverse Methods. *Methods of soil analysis: Part 4 Physical methods*, *5*, 963-1008.

Hudson, D.B., Young, M.H., Wierenga, P.J., and Hills, R.G. (1991). Transient method for estimating soil water parameters of unsaturated soil cores. P. 221. In Agronomy Abstracts. ASA, Madison, WI.

IPCC, 2007: Climate Change 2007: Impacts, Adaptation and Vulnerability. Contribution of Working Group II to the Fourth Assessment Report of the Intergovernmental Panel on Climate Change, M.L. Parry, O.F. Canziani, J.P. Palutikof, P.J. van der Linden and C.E. Hanson, Eds., Cambridge University Press, Cambridge, UK, 976pp.

Isch, A., Coquet, Y., Abbar, B., Aldana, C., Abbas, M., Bruand, A., and Azaroual, M. (2022). A comprehensive experimental and numerical analysis of water flow and travel time in a highly heterogeneous vadose zone. *Journal of Hydrology*, *610*, 127875.

Al-Kaisi, M. (2017). How droughts affects soil health, Integrated crop management news, Iowa State University Extension and Outreach.

Kanzari, S., Ben Nouna, B., Ben Mariem, S., and Rezig, M. (2018). Hydrus-1D model calibration and validation in various field conditions for simulating water flow and salts transport in a semi-arid region of Tunisia. Sustainable Environment Research, 28(6), 350–356. https://doi.org/10.1016/j.serj.2018.10.001

Kirkham, M.B. (2023). Principles of Soil and Plant Water Relations. Academic Press.

Kool, J.B., Parker, J.C. and Van Genuchten, M.Th., 1987. Parameter estimation for unsaturated flow and transport models -- A review. J. Hydrol., 91: 255-293.

Kosugi K. (1996). Lognormal distribution model for unsaturated soil hydraulic properties, *Water Resour. Res.*, *32*(9), 2697-2703

Kubinec, A. (2018). Building a 'Better' Crop Rotation. Manitoba Agriculture, 1. Assessed: May 01, 2024.

Kurt G. (2023). Agricultural and Agri-Food Sciences. Personal Communication.

Lee, D. M., Elrick, D. E., Reynolds, W. D., and Clothier, B. E. (1985). A comparison of three field methods for measuring saturated hydraulic conductivity. *Canadian journal of soil science*, *65*(3), 563-573.

Legates, D. R., and McCabe, G. J. (1999). Evaluating the use of "goodness-of-fit" measures in hydrologic and hydroclimatic model validation. Water Resources Res. 35(1): 233-241.

Leonard, R.A.; Knisel, W.G.; Still, D.A. (1987). GLEAMS: Groundwater loading effects of agricultural management systems. Trans. ASAE, 30, 1403–1418.

Manitoba Agriculture, (2010). Soil Series Description.

Manitoba Agricultural Services Corporation., 2021. Annual Report 2020-2021. www.masc.mb.ca/masc.nsf/annual_report_2020_21.pdf

Manitoba Agriculture, (2019). Manitoba Protein Research Strategy. Assessed: April 26, 2024 https://www.manitoba.ca/agriculture/protein/advantage-strategyAAFC. Sustainable Canadian Agricultural Partnership

Manitoba Agriculture, (2021). Census of Agriculture, 2021.

Manitoba Agriculture, (2023). Sector profile at a glance Agriculture.

Manitoba Agriculture, (2023). The Manitoba Advantage in Oats.

Manitoba Agriculture, (2024a). Sector profile at a glance Agriculture.

Manitoba Agriculture, (2024b). Sector profile at a glance Soybean.

Manitoba Agriculture, (2024c). Sector profile at a glance Oats.

Manitoba Agriculture, (2024d). Climate Change in Manitoba.

Manitoba Agriculture, (2024e). Raw Commodities and Primary Agriculture. Assessed: July 30, 2024

Manitoba Crop Alliance (2024). Extremes of Moisture. Assessed: July 30, 2024.

Manitoba Forestry Association. (2008). The proposed soil of Manitoba - The newdale soil.

Mante, A.A., and Sri Ranjan, R. (2017). HYDRUS (2D/3D) simulation of water flow through sandy loam soil under potato cultivation in southern Manitoba. Canadian Biosystems Engineering, 59, 1.9-1.19.

Mante, A.A., Sri Ranjan, R., Bullock, P. (2018). Subsurface drainage for promoting soil strength for field operations in southern Manitoba. Soil Till. Res., 184, 261–268

Marquardt, D.W. (1963) An Algorithm for Least Squares Estimation of Nonlinear Parameters. Journal of the Society for Industrial and Applied Mathematics, 11, 431-441.

McKenzie, N., Coughlan, K., and Cresswell, H. (2002). *Soil physical measurement and interpretation for land evaluation*. CSIRO Pub.

McKenzie, R.H. (2010). Agricultural Soil Compaction: Causes and Management. Government of Alberta.

Merrill, S., Schuster-Wallace, C. J., DeBeer, C., and Sandford, R. (2019). Water Futures for the World We Want: State of Global Water Futures Methods, Models and Data. *University of Saskatchewan, Saskatoon, Canada This report content was originally published as: Merrill, S., Schuster-Wallace, CJ, and Sandford*.

Mills, G.F., Haluschak, P. (1993). Soils of the Carman Research Station. CANADA-MANITOBA Soil Survey Spec Report Ser 93-1 [Internet]

Moges, E., Demissie, Y., Larsen, L., and Yassin, F. (2021). Sources of hydrological model uncertainties and advances in their analysis. *Water*, *13*(1), 28.

Moriasi, D. N., Arnold, J. G., Van Liew, M. W., Bingner, R. L., Harmel, R. D., and Veith, T. L. (2007). Model evaluation guidelines for systematic quantification of accuracy in watershed simulations. *Transactions of the ASABE*, *50*(3), 885-900.

Mualem, Y. (1976). A new model for predicting the hydraulic conductivity of unsaturated porous media, *Water Resour. Res., 12*(3), 513-522

Müller, M., Schneider, J. R., Klein, V. A., da Silva, E., da Silva Júnior, J. P., Souza, A. M., and Chavarria, G. (2021). Soybean Root Growth in Response to Chemical, Physical, and

Biological Soil Variations. Frontiers in plant science, 12, 602569. https://doi.org/10.3389/fpls.2021.602569

Ndulue, E.L. (2022). Water management of Canola under tile drainage in the Canadian Prairies. PhD Thesis, Department of Biosystems Engineering, University of Manitoba.

Ojo, E.R. (2017). In situ and Modelled Soil Moisture Determination and Upscaling from Point-based to Field Scale. PhD Thesis. Department of Soil Science, University of Manitoba.

Osborne, S. L., Riedell, W. E., Schumacher, T. E., and Humburg, D. S. (2003). Use of cover crops to increase corn emergence and field trafficability. *Soil/Water Research, Progress Report*, 2-39.

Pacheco, A., L'Heureux, J., Mcnairn, H., Powers, J., Howard, A., Geng, X., Gottfried, K., Freeman, J., Ojo, R., Champagne, C., Rodgers, E., Smith, C., Fitzmaurice, J., Merzouki, A., Hansen, T., Wyryha, B., Chubey, M., and Einarsson, E. (2014). Real-Time In-Situ Soil Monitoring for Agriculture (RISMA) Network Metadata. http://aafc.fieldvision.ca/application/web_assets/files/RISMA_Network_Metadata.pdf

PAMI. (2018). Beneficial Management Practices for Agricultural Tile Drainage in Manitoba. Assessed: July 28, 2024

Patel, K. F., Fansler, S. J., Campbell, T. P., Bond-Lamberty, B., Smith, A. P., Roychowdhury, T., McCue, L. A., Varga, T., and Bailey, V. L. (2021). Soil texture and environmental conditions influence the biogeochemical responses of soils to drought and flooding. Communications Earth and Environment, 2(2021), 1–9. https://doi.org/10.1038/s43247-021-00198-4

Pechlivanidis, I. G., Jackson, B. M., Mcintyre, N. R., and Wheater, H. S. (2011). Catchment scale hydrological modelling: A review of model types, calibration approaches and uncertainty analysis methods in the context of recent developments in technology and applications. *Global NEST journal*, *13*(3), 193-214.

Pierce, B., Ignaszewski, E., Gertner, D., Leet-Otley, T. (2024). U.S. retail market insights for the plant-based industry. Date assessed: July 22, 2024

Poeter, Eileen P., Hill, Mary C. (1999) UCODE, a computer code for universal inverse modeling. Computers and Geosciences, Volume 25, Issue 4, Pages 457-462,ISSN 0098-3004, https://doi.org/10.1016/S0098-3004(98)00149-6.

Powers, J. (2014). Re-Installation of Hydra-Probes at RISMA Station MB 5, Agriculture and Agri-Food Canada, Winnipeg, MB, 6pp.

Province of Manitoba. (2021). Economic Impacts of the 2021 Drought on Crop Production in Manitoba.

Qian, B., Bonsal, B., Jing, Q., Smith, W. N., Jégo, G., Zhang, Y. Crépeau, M. (2024). The potential of growing soybean in Saskatchewan and its irrigation water needs under climate change scenarios – a modelling study. Canadian Journal of Plant Science. https://doi.org/10.1139/cjps-2023-0148

Qiao S. Y. 2014. Modeling water flow and phosphorus fate and transport in a tile-drained clay loam soil using HYDRUS (2D/3D). MSc. Thesis. McGill University, Canada.

Rabbi, S.M.F., Tighe, M.K., Warren, C.R., Zhou, Y., Denton, M.D., Barbour, M.M., Young, I.M. (2021). High water availability in drought tolerant crops is driven by root engineering of the soil micro-habitat. Geoderma, Volume 383.

Ragab, R. Malash, N. Abdel Gawad, G. Arslan, A. Ghaibeh (2005). A holistic generic integrated approach for irrigation, crop, and field management: 1. The SALTMED model and its calibration using field data from Egypt and Syria

Ramos, T. B., J. Šimůnek, M. C. Gonçalves, J. C. Martins, A. Prazeres, N. L. Castanheira, and L. S. Pereira. 2011. Field evaluation of a multicomponent solute transport model in soils irrigated with saline waters. J. Hydrol. 407(1-4): 129-144.

Riedy, C. (2016). Climate Change. Blackwell Encyclopedia of Sociology. Blackwell.

RoTimi Ojo, E., and Manaigre, L. (2021). The Manitoba Agriculture Mesonet. Bulletin of the American Meteorological Society, 102(9), 1786–1804.

Sadras, V. O., Villalobos, F. J., Orgaz, F., and Fereres, E. (2016). Principles of Agronomy for Sustainable Agriculture. Principles of Agronomy for Sustainable Agriculture.

Satchithanantham, S., Sri Ranjan, R., and Shewfelt, B. (2012). Effect of water table management and irrigation on potato yield. Transactions of ASABE 55(6):2175-2184.

Sauchyn, D. and Kulshreshtha, S. (2008): Prairies; From Impacts to Adaptation: Canada in a Changing Climate 2007, edited by D.S. Lemmen, F.J. Warren, J. Lacroix and E. Bush; Government of Canada, Ottawa, ON, p.275-328.

Schaap, M. G., Leij, F. J., and Van Genuchten, M. T. (2001). Rosetta: A computer program for estimating soil hydraulic parameters with hierarchical pedotransfer functions. *Journal of hydrology*, *251*(3-4), 163-176.

Shaheb, M.R., Venkatesh, R. and Shearer, S.A. A Review on the Effect of Soil Compaction and its Management for Sustainable Crop Production. *Journal of Biosystems. Engineering.* **46**, 417–439 (2021)

Setiyono, T. D., Weiss, A., Specht, J. E., Cassman, K. G., and Dobermann, A. (2008). Leaf area index simulation in soybean grown under near-optimal conditions. *Field Crops Research*, *108*(1), 82-92.

Šimůnek, J., and De Vos, J. A. (1999). Inverse optimization, calibration and validation of simulation models at the field scale. *Modelling of Transport Process in Soils at Various Scales in Time and Space*, 431-445.

Šimůnek, J., and Hopmans, J.W. (2002). Chapter 1.7: Parameter Optimization and nonlinear Fitting. In Methods of Soil Analysis: Part 1: Physical methods, 139-157. J.H. Dane and G.C. Topp, eds. 3rd Edition. Madison, Wisc.: SSSA.

Šimůnek, J. (2008). Residual water content. PC-Progress Discussion Forums, HYDRUS-1D. Assessed: July 24, 2024. https://www.pc-progress.com/forum/viewtopic.php?t=1150

Šimůnek, J.; Šejna, M.; Saito, H.; Sakai, M.; van Genuchten, M.T. (2013). The HYDRUS-1D Software Package for Simulating the One-Dimensional Movement of Water, heat, and Multiple Solutes in Variably-Saturated Media Version 4.17; University of California Riverside: Riverside, CA, USA.

Šimůnek, J., Šejna, M., and van Genuchten, M.T. (2018). New Features of the Version 3 of the HYDRUS (2D/3D) Computer Software Package, Journal of Hydrology and Hydromechanics, 66(2), 133-142

Singh, V.P. and Woolhiser, D.A. (2002) Mathematical Modelling of Watershed Hydrology. Journal of Hydrological Engineering, ASCE, 7, 270-292.

Soy Canada. (2023). Annual Report.

Statistics Canada. (2023). The Prairies, Quebec lead the way in high-tech farm management. Assessed: July 24, 2024.

Statistics Canada. (2023). The socioeconomic snapshot of Canada's evolving farm population, 2021. Assessed: February 2024.

Statistics Canada. (2016). Land and freshwater area, by province and territory. Table 15.7. Date assessed: July 23,2024.

Statistics Canada. (2024). Land use, Census of Agriculture historical data. Table 32-10-0153-01. Assessed: May07, 2024.

Statistics Canada. (2023). Estimated areas, yield, production, average farm price and total farm value of principal filed crops, in metric and imperial units. Date assessed: March 23, 2024.

Staton, M. (2014). Irrigation Water Management and Soybean Diseases. Michigan State University Extension.

Stewart, R. D., M. R. Abou Najm, D. E. Rupp, and J. S. Selker (2016), Modeling multidomain hydraulic properties of shrink-swell soils, Water Resour. Res., 52, 7911–7930, doi:10.1002/2016WR019336.

Suleiman, A. A. (2008). Modeling daily soil water dynamics during vertical drainage using the incoming flow concept. *Catena*, *73*(3), 312-320.

Suarez D.I., Šimůnek J. (1997). UNSATCHEM: unsaturated water and solute transport model with equilibrium and kinetic chemistry

Tan, C. S., Drury, C. F., Ng, H. Y. F. and Gaynor, J. D. 1999. Effect of controlled drainage and sub-irrigation on subsurface tile drainage

The Senate of Canada. (2024). Critical ground: why soil is essential to Canada's economic, environmental, human, and social health. A report of the Standing Senate Committee on Agriculture and Forestry. Assessed: July 28, 2024

Tolson, B. A., and Shoemaker, C. A. (2008). Efficient prediction uncertainty approximation in the calibration of environmental simulation models. Water Resources Research, 44(4).

University of Manitoba. (2024). Sustainability courses for UM students, Education and Research. Date assessed: July 22, 2024

Van Dam, J.C., Huygen, J., Wesseling, J.G., Feddes, R.A., Kabat, P., van Walsum, P.E.V., Groenendijk, P., van Diepen, C.A. (1997). Theory of SWAP Version 2.0: Simulation of Water Flow, Solute Transport and Plant Growth in the Soil-Water-Atmosphere-Plant Environment; Technical Document 45; Wageningen Agricultural University and DLO Winand Staring Centre: Wageningen, The Netherlands.

van Genuchten, M. Th. (1980). A closed-form equation for predicting the hydraulic conductivity of unsaturated soils, *Soil Sci. Soc. Am. J., 44*, 892-898

Vogel, T., and Císlerová, M. (1988). On the reliability of unsaturated hydraulic conductivity calculated from the moisture retention curve, *Transport in Porous Media, 3*, 1-15.

Voora, V., Bermudez, S., Le, Han., Larrea, C., Luna, E. (2024). Global Market Report: Soybean prices and sustainability. International Institute for Sustainable Development.

Walker, B.D. (2012). Agri-Environmental Monitoring – Manitoba: Methodology and landscape descriptions. Agriculture and Agri-Food Canada, Agri-Environmental Services Branch. Winnipeg, MB and Ottawa, ON. 29 pp.

Wang X. (2018). Numerical Assessment of Evapotranspiration Covers in Cold Climates. M.Sc. Thesis. University of Manitoba, Canada

Warrick, A.W. and Nielsen, D.R. (1980) Spatial Variability of Soil Physical Properties in the Field. In: Hillel, D., Ed., Applications of Soil Physics, Academic Press, New York.

Watson, C.A. et al., (2002). Managing soil fertility N organic farming systems. Soil Use and Management, 18, 239-247.

Wichers, G. (2019). Soil degradation a costly global issue. Farmit Manitoba. Local news. Assessed July 30, 2024.

Wilding, L., and Drees, L.R. (1983) Spatial Variability and Pedology. In: Developments in Soil Science, Elsevier, Amsterdam, 83-116.

Woessner, William W. and Eileen P. Poeter 2020, Hydrogeologic Properties of Earth Materials and Principles of Groundwater Flow. The Groundwater Project, Guelph, Ontario, Canada.

Yang L. 2021. Crop yield impacts from rotations in Manitoba. M.Sc. Thesis. University of Manitoba, Canada.

Zhang K., Ruben G. B., Li X., Li Z., Yu Z., Xia J., et al. (2020). A comprehensive assessment framework for quantifying climatic and anthropogenic contributions to streamflow changes: a case study in a typical semi-arid North China basin. *Environ. Modell. Softw.* 128:104704. 10.1016/j.envsoft.2020.104704